



Hydrologic, biogeochemical, microbial, and macroinvertebrate responses to network expansion, contraction, and disconnection across headwater stream networks with distinct physiography in Alabama, USA

- Stephen Plont¹, Delaney M. Peterson¹, Chelsea R. Smith¹, Charles T. Bond², Andrielle Larissa Kemajou Tchamba³, Michelle A. Wolford¹, Kaci Zarek^{1,4}, Shannon L. Speir⁵, C. Nathan Jones¹, Jonathan P. Benstead¹, Michelle H. Busch^{6,7}, Rebecca L. Hale⁸, Connor L. Brown⁶, Erin C. Seybold⁶, Arial J. Shogren¹, Kevin A. Kuehn², Yaqi You⁹, Colin R. Jackson³, Amy J. Burgin¹⁰, Carla L. Atkinson¹
 - ¹Department of Biological Sciences, University of Alabama, Tuscaloosa, Alabama, 35487, USA
- ²School of Biological, Environmental, and Earth Sciences, University of Southern Mississippi, Hattiesburg, Mississippi, 39406, USA
 - ³Department of Biology, The University of Mississippi, Oxford, Mississippi, 38677, USA
 - ⁴Department of Ecology and Evolutionary Biology, Cornell University, Ithaca, New York, 14850, USA
 - ⁵Department of Crop, Soil, and Environmental Sciences, University of Arkansas, Fayetteville, Arkansas, 72701, USA
- 15 ⁶Kansas Geological Survey, Department of Geology, University of Kansas, Lawrence, Kansas, 66045, USA
 - ⁷Michigan Natural Features Inventory, Michigan State University Extension, Lansing, Michigan, 48901, USA
 - ⁸Smithsonian Environmental Research Center, Edgewater, Maryland, 21037, USA
 - ⁹Department of Environmental Resources Engineering, The State University of New York College of Environmental Science and Forestry, Syracuse, New York, 13210, USA
- 20 ¹⁰Department of Ecology, Evolution, and Organismal Biology, Iowa State University, Ames, Iowa, 50011, USA

Correspondence to: Stephen Plont (plontste@gmail.com)

Abstract. Here we present a comprehensive dataset of hydrologic, biogeochemical, microbial, and macroinvertebrate community measurements from a set of multi-year, co-occurring, watershed studies in non-perennial stream networks that dynamically expand and contract over space and time. The data were collected over the 2022-2024 water years across three stream networks draining watersheds with a similar humid, subtropical climate but distinct physiographies (i.e., Piedmont, Appalachian Plateau, Coastal Plain) in Alabama, USA. Our goal was to characterize the spatiotemporal patterns and drivers of how non-perennial stream networks expand and contract, as well as the biogeochemical, microbial, and macroinvertebrate dynamics associated with changes in network connectivity and water availability. We used a combination of spatial, temporal, and spatiotemporal sampling and sensor-based monitoring approaches to capture hydrologic, biogeochemical, and ecological responses to network expansion and contraction in each watershed. This manuscript describes the overall study design, monitoring network and sampling approaches, data and sample collection and analysis, and specific datasets generated. All data products are publicly available through the Hydroshare data repository for hydrologic, biogeochemical, and macroinvertebrate data (https://www.hydroshare.org/group/247) and through the NCBI data repository for microbial data. All data product-specific DOIs and repository-specific unique IDs are cited in Appendix A (Table A1, Table A3).





1 Introduction

40

45

Non-perennial streams, or streams that cease flowing throughout the year (also known as intermittent rivers and ephemeral streams, IRES; Busch et al., 2020), are ubiquitous, making up over half of global stream miles (Messager et al., 2021). Despite their ephemeral connectivity to permanent water bodies, non-perennial streams contribute over half of the streamflow on average to downstream river systems in the United States (Brinkerhoff et al., 2024), generate unique biogeochemical and ecological signals compared to perennial streams (Bernal et al., 2022; Gómez-Gener et al., 2021; López-Rojo et al., 2025; Zarek et al., 2025), and serve as important determinants of downstream water quality, biodiversity, and ecosystem services (Datry et al., 2023; Gómez et al., 2017; Marcé et al., 2019; Meyer et al., 2007). Climate change is altering the timing and severity of large storms and droughts, leading to unprecedented shifts in the geographic extent and hydrologic regimes of non-perennial streams (Tramblay et al., 2021; Zipper et al., 2021), highlighting the need to include these vulnerable ecosystems in policy and regulatory frameworks (Lane et al., 2023; Walsh and Ward, 2022). However, non-perennial streams remain largely absent from streamflow and water-quality monitoring networks (Krabbenhoft et al., 2022), hindering our ability to study downstream consequences of changing flow and connectivity dynamics in non-perennial streams. Further, given the temporal variability and spatial complexity of non-perennial streams, we must also look upstream of the watershed outlet and utilize coordinated, interdisciplinary approaches to understand the patterns and drivers of network-scale connectivity, biogeochemistry, and ecology in non-perennial systems (Bernal et al., 2025; Zimmer et al., 2022).

Contextualizing the role of non-perennial streams in freshwater network processes requires further representation of non-perennial stream networks in watershed-scale studies. However, watershed-scale studies often experience trade-offs between assessing temporal variation and spatial heterogeneity, both of which are needed to fully understand hydrologic, biogeochemical, and ecological patterns in non-perennial stream networks. Many watershed studies utilize long-term monitoring approaches that are fixed-in-space but allow for temporal assessment of watershed processes such as water yield and material export. Our understanding of watershed-scale hydrologic and ecological processes has also advanced greatly with the advent of lower-cost, high-frequency environmental sensor technology and advances in ecosystem modeling approaches (Bieroza et al., 2023; Blaen et al., 2016; Ruhala and Zarnetske, 2017). However, these outlet-only approaches miss the opportunity to study phenomena that are driven by spatial heterogeneity within the watershed, such as the routing and connectivity of water and materials to the stream network (Ward et al., 2019b), spatial patterns of biodiversity (Poff, 1997; Rolls et al., 2018; Ruhí et al., 2017), and local changes to biogeochemical processes that ultimately drive signals at the watershed outlet (Abbott et al., 2018). Spatially extensive, "synoptic" sampling studies directly complement watershed outlet monitoring by attempting to capture a fixed-in-time snapshot of the stream network and to allow for empirical assessment of spatial patterns of sources, connectivity, processes, and biodiversity. Co-collection of hydrologic, biogeochemical, and ecological data during synoptic campaigns can provide an integrated perspective on the importance of different ecosystem patches that contribute disproportionately as material sources and sinks, habitat, and species diversity (Shogren et al., 2022; Ward et al., 2019a). However, the spatial patterns observed by these synoptic approaches are limited in their scope and power





to assess antecedent drivers. These issues are particularly apparent in non-perennial stream networks, as spatial patterns of water persistence and connectivity, sources and fate of solutes and materials, and biodiversity and food web energy flow are influenced by interannual, seasonal, and event-scale variability in streamflow, network extent, and environmental phenology.

The data presented herein represent a substantial and novel effort to characterize how spatial and temporal patterns of flow and connectivity throughout non-perennial stream networks drive watershed-scale biogeochemical and ecological responses. Using a combination of sampling and sensor-based monitoring approaches, we aimed to capture concurrent hydrologic, biogeochemical, and ecological responses to stream network expansion and contraction across three study watersheds in Alabama, USA. These watersheds span three distinct physiographies - Piedmont, Appalachian Plateau, and Coastal Plain - and vary in terms of their watershed geology, vegetation, and network topology, despite experiencing a similar climate. Throughout each stream network and over the course of three consecutive water-years (Autumn 2021-Autumn 2024), we collected continuous water presence-absence (Stream Temperature Intermittency and Conductivity or STICs; n = 20 sites per watershed) and water-level data (long term monitoring sites; n = 7 sites per watershed) and conducted seasonal synoptic sampling campaigns to capture spatiotemporal biogeochemical and ecological conditions. At each watershed outlet (supersensor; n = 1), we measured water quality parameters continuously and collected water chemistry samples tri-weekly. Lastly, we conducted a single, spatially extensive synoptic sampling campaign in our focal Piedmont watershed in June 2022 to gain a spatially resolved understanding of biogeochemical and ecological dynamics. Together, this comprehensive dataset consisting of both high-resolution temporal and spatial sampling and monitoring approaches provides valuable context as to how changes in stream flow and connectivity drive hydrologic, biogeochemical, and ecological patterns in non-perennial streams in the southeastern USA.

Table 1: Summary of watershed characteristics and dates for sampling approach 2 and 3 campaigns. Bolded dates denote the sampling approach 3 campaign and asterisks denote "bonus" sampling approach 2 campaigns. These bonus sampling campaigns are only in one watershed and have limited data coverage (e.g., no microbial or macroinvertebrate data).

	Piedmont (TAL)	Appalachian Plateau (PRF)	Coastal Plain (WHR)
Outlet Coordinates	33.762197°, -85.595507°	34.968617°, -86.165017°	32.984109°, -88.013343°
Drainage Area (km²)	0.92	2.97	0.7
Elevation Range (m)	345 - 456	211 - 550	63 - 94
Median Channel Slope	2.5	5.9	0.8
Median TWI	13.9	16.4	15.6
Geologic Setting	low-grade fractured metamorphic rocks	karstic sedimentary rocks	sedimentary marine deposits
Approach 2 and 3 Sampling Dates	2022: 1/24-1/25*, 3/29-3/30, 6/9-6/10 , 8/11-8/12; 2023: 1/30-1/31, 5/16, 8/7, 11/27*; 2024: 1/29	2022: 3/13-3/14, 8/23-8/24; 2023: 2/13-2/14, 4/24-4/25, 7/24-7/25; 2024: 2/19-2/20	<u>2022</u> : 3/24, 8/15; <u>2023</u> : 2/7, 5/9, 8/1; <u>2024</u> : 1/22

100

2 Study location and sampling design

2.1 Study watersheds

We selected three study watersheds in the state of Alabama that were representative of the physiographic gradient in the southeastern USA (Table 1, Fig. 1). All three watersheds were relatively comparable in size and received similar precipitation inputs in a humid subtropical climate setting. Below, we describe the primary geologic, hydrologic, topographic, and vegetative characteristics of each watershed.

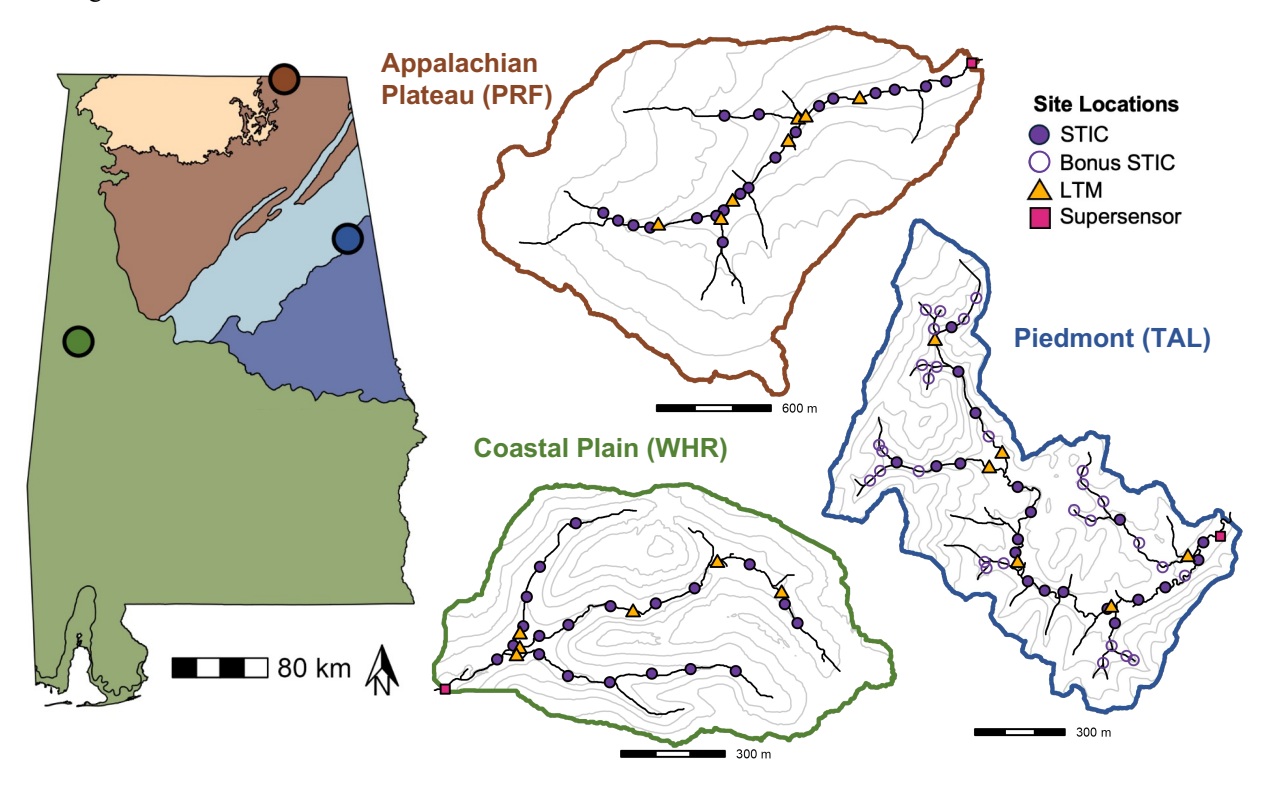


Figure 1: (left) Map of Alabama, USA with locations of the three study watersheds. Points shown on the Alabama map as well as the outlines of the Piedmont (Talladega: TAL; right, blue), Appalachian Plateau (Paint Rock: PRF; top, brown), and Coastal Plain (Shambley Creek: WHR; bottom, green) study watersheds are colored based on their respective physiographic province. Locations of water presence-absence sensors (STIC; purple circles), long-term monitoring sites (LTM; gold triangles), and watershed outlet monitoring sites (Supersensor; pink squares) in the stream network are shown on each watershed map (see Section 2.2.1). Additional water presence-absence sensors (Bonus STIC; open circles with purple outline) were installed in the Piedmont study watershed during 2022 to correspond with sites sampled during a spatially-intensive synoptic sampling campaign in June (sampling approach 3; Section 2.2.4).

2.1.1 Piedmont

105

110

Our focal study watershed in the Piedmont physiographic province is a 0.92-km² watershed within the larger Talladega National Forest (TAL; Table 1, Fig. 2). This watershed is completely forested and located within federally owned



120

125

130

135

public lands (953 km²) managed primarily for recreation, conservation, and silviculture. The watershed has moderate topographic relief with elevation ranging from 345 to 456 meters above sea level (hereafter, masl) and forms an unnamed non-perennial tributary to Pendergrass Creek in Cleburne County (AL, USA), which drains to the Coosa River within the Mobile-Tombigbee basin. Geologically, this watershed is underlain by low-grade metamorphic rocks, primarily interbedded phyllite, metasiltstone, and quartzite units that are heavily fractured due to their proximity to the Talladega fault (Szabo et al., 1988; Cook, 1982; Kopaska-Merkel, et al., 2000). The soils in this watershed are predominantly highly weathered Ultisols, with thin, rocky slopes in the headwaters compared to more organic, fine-grained soils near the outlet (Soil Survey Staff, 2025; Zarek et al., 2025). The dominant vegetation type in the region is oak-hickory-pine, and the watershed is a mixed deciduous-coniferous forest with primarily pine (loblolly, longleaf) and oak (mixed red and white) species (Griffith et al, 2001; Feminella, 1996). Additionally, this watershed experiences low-intensity prescribed burns for habitat management, including in the early spring of both 2022 and 2024 during our study.

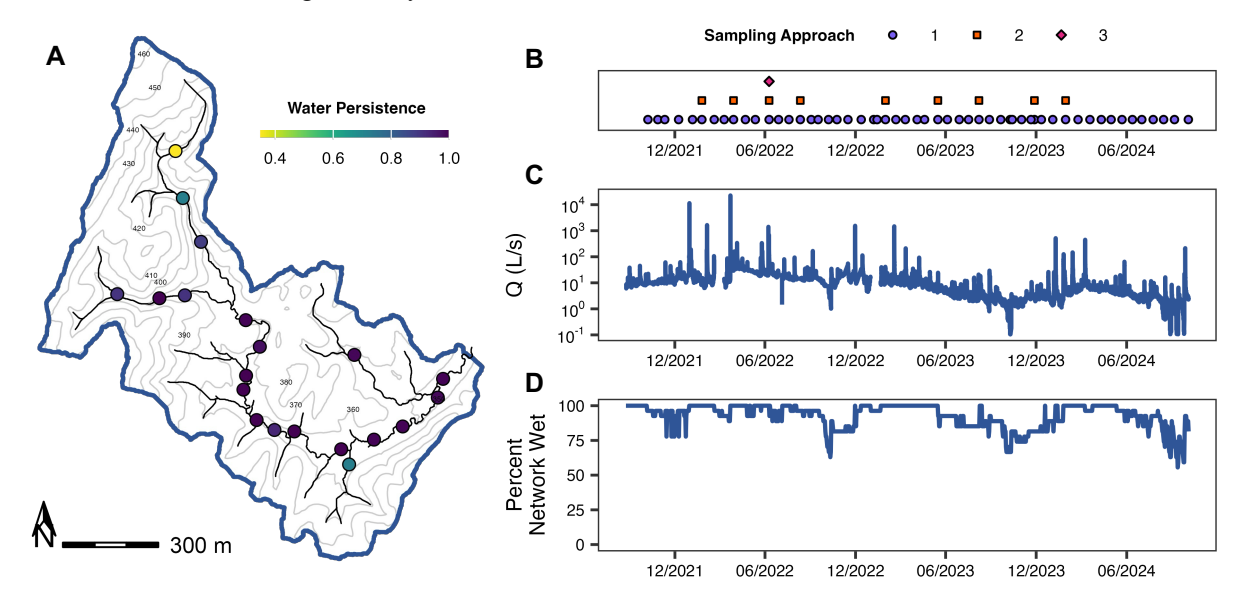


Figure 2: (A) Flow persistence over the study period (September 2021-October 2024) at each water presence-absence sensor site across the Piedmont study watershed. Light colors indicate less water persistence and darker colors indicate continuous water persistence. (B) Sampling dates, (C) discharge at the watershed outlet (Q; L s⁻¹) and (D) percent network wet (see Section 3.2.2 for further details) across the study period. For a given sampling date, purple circles refer to temporal sampling at the watershed outlet (sampling approach 1; Section 2.2.2) and orange squares for seasonal synoptic sampling at the seven long-term monitoring sites in the stream network (sampling approach 2; Section 2.2.3) and pink diamonds for an intensive spatial synoptic sampling campaign across the watershed (sampling approach 3; see Section 2.2.4).

2.1.2 Appalachian Plateau

Our study watershed in the Appalachian Plateau physiographic province, Paint Rock (PRF), is a 2.97-km² watershed in Jackson Country, AL (USA; Table 1, Fig. 3). Almost entirely forested, the Appalachian Plateau watershed is privately



145

150

155

160

owned and managed for recreation and conservation. This watershed drains Miller Mountain and Fanning Hollow to form an unnamed tributary to Burks Creek, located within the Paint Rock River and larger Tennessee River basins. This is the highest relief watershed with elevation ranging from 211 to 550 masl. Geologically, this watershed is underlain by karst sedimentary rocks, primarily sandstones interbedded with shales, limestone, dolomite, and mudstones (Szabo et al., 1988), and the headwaters are located in the exposure of the limestone unit that yields the majority of caves and karst features in the state (Ponta, 2018). Due to the steep slopes, the watershed mostly contains thin, stony soils within the Ultisol and Mollisol soil orders (Soil Survey Staff, 2025). Most soil formation and sediment accumulation occurs in the lower portion of the network, with exposed bedrock benches forming the stream channels in the headwaters (Soil Survey Staff, 2025). The forest community is primarily deciduous, with dominant vegetation types of mixed oaks (chestnut, red, and white) in the upper slopes, mesic forest (beech, yellow poplar, sugar maple, basswood, ash, and buckeye) in the middle and lower slopes, and riparian zones with river birch and hemlock (Griffith et al., 2001).

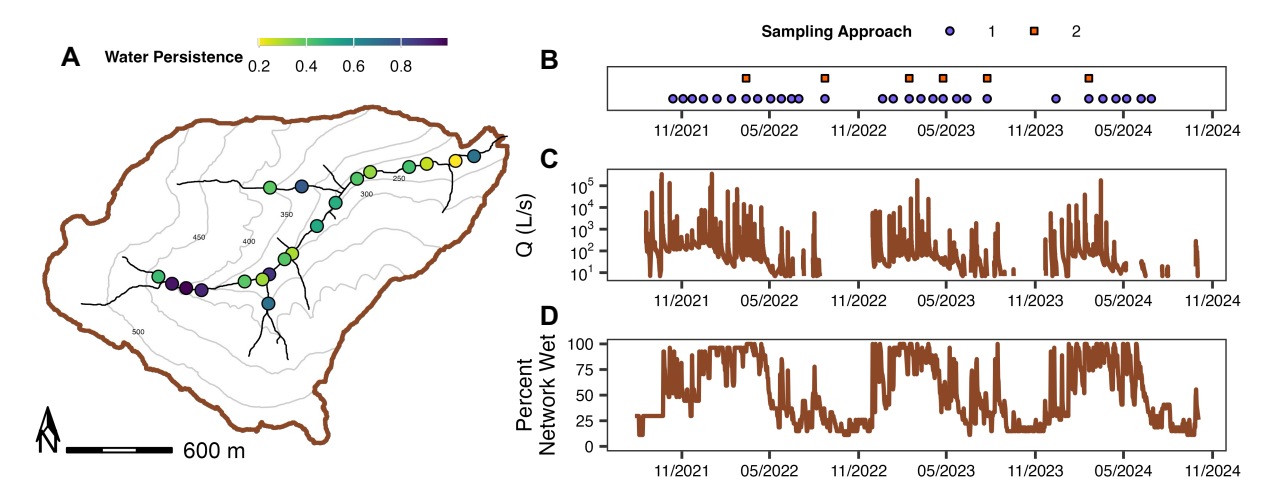


Figure 3: (A) Flow persistence over the study period (August 2021-October 2024) at each water presence-absence sensor site across the Coastal Plain study watershed. Light colors indicate less water persistence and darker colors indicate continuous water persistence. (B) Sampling dates, (C) discharge at the watershed outlet (Q; L s⁻¹) and (D) percent network wet (see Section 3.2.2 for further details) across the study period. For a given sampling date, purple circles refer to temporal sampling at the watershed outlet (sampling approach 1; Section 2.2.2) and orange squares for seasonal synoptic sampling at the seven long-term monitoring sites in the stream network (sampling approach 2; Section 2.2.3).

2.1.3 Coastal Plain

Our study watershed in the Coastal Plain physiographic province, Shambley Creek (WHR), is a 0.70-km² watershed in Greene County, AL (USA; Table 1, Fig. 4). This watershed is completely forested and is privately owned and managed for rotational silvicultural harvest by the Weyerhaeuser Company. This watershed forms the unnamed headwaters of Shambley Creek, which drains to the Sipsey River in the larger Mobile-Tombigbee basins. This is the lowest relief watershed with elevation ranging from 63 to 94 masl. Geologically, this watershed is underlain by sedimentary units, primarily interbedded clay and sand layers that are one of the integral water-bearing units in the region (Szabo et al., 1988). This soils in this watershed



170

175

180

185

190

are predominantly highly-weathered Ultisols, and the low relief paired with easily erodible soil textures has resulted in highly incised channels in the lower half of the watershed. This region has a historic forest structure of mixed coniferous and deciduous species (oaks, hickory, and pine species; Griffiths et al., 2001). However, in this watershed, the upland areas are almost entirely pine with dense riparian species (i.e., gum, holly, sycamore, ironwood). The southern portion of this watershed was thinned in the summer of 2024, but the harvest only occurred in the upland areas (i.e., all forest within ~8 m of the channel was preserved).

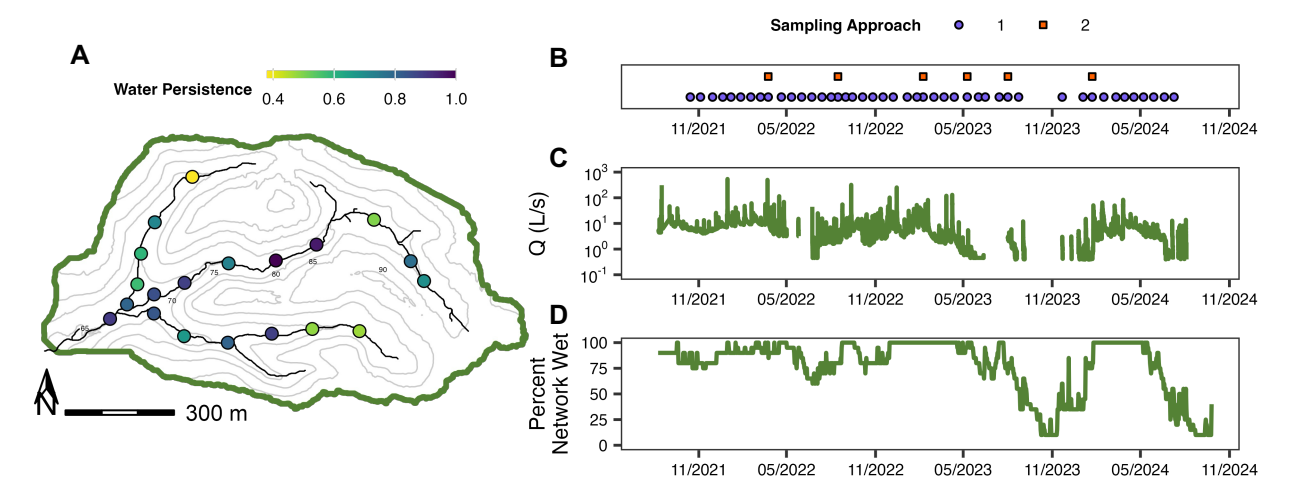


Figure 4: (A) Water persistence over the study period (August 2021-October 2024) at each water presence-absence sensor site across the Coastal Plain study watershed. Light colors indicate less water persistence and darker colors indicate continuous water persistence. (B) Sampling dates, (C) discharge at the watershed outlet (Q; L s⁻¹) and (D) percent network wet (see Section 3.2.2 for further details) across the study period. For a given sampling date, purple circles refer to temporal sampling at the watershed outlet (sampling approach 1; Section 2.2.2) and orange squares for seasonal synoptic sampling at the seven long-term monitoring sites in the stream network (sampling approach 2; Section 2.2.3).

2.2 Watershed sampling design

2.2.1 Sensor monitoring networks

Within each study watershed, we deployed high spatial-resolution sensor monitoring networks that maximized continuous data collection with multiple data types (Table 2). These monitoring networks were developed using a standardized site design that targeted both key locations within the network (i.e., tributary confluences, the watershed outlet) and randomly distributed sites across a gradient of topographic conditions (Swenson et al., 2024; Zipper et al., 2025a). Altogether, integrating across these different sensor types and network locations provides both the context of hydrologic connectivity and the downstream water-quality consequences for the rest of this project. The different components of these sensor networks can be divided into three categories: 1) multi-parameter water quality sondes located at the watershed outlet (supersensor; n = 1 site per watershed), 2) long-term monitoring (LTM) sites consisting of in-stream stilling wells and piezometers instrumented with pressure transducers (n = 7 sites, including the watershed outlet), 3) water presence-absence sensors throughout the watershed





(STICs; n = 20 sites, including the watershed outlet). We also deployed and maintained local weather stations recording barometric pressure, rainfall, temperature, relative humidity, wind direction and speed, and photosynthetically active radiation (PAR). All weather stations were located in the nearest open-canopy location within 5 km of the watershed outlet, though both the Appalachian Plateau and Coastal Plain locations were within 1 km of their respective watershed outlet.

Table 2: Summary of time series data products collected in the Piedmont (TAL), Appalachian Plateau (PRF), and Coastal Plain (WHR) watersheds.

Data Product	Parameter	Units	Data Product Citation Identifier (See Table A1)			
			Piedmont (TAL)	App. Plateau (PRF)	Coastal Plain (WHR)	
Site Information and	Latitude, Longitude	DD	TAL_ENVI	PRF_ENVI	WHR_ENVI	
Watershed Characteristics	Elevation	masl				
(ENVI)	TWI					
	Distance from outlet	m				
	Drainage area	m^2				
	Slope (at point)	degrees				
	Slope (in a 5-m buffer)	degrees				
	Slope (in a 25-m reach)	degrees				
Meteorological (METS)	Temperature	°C	TAL METS	PRF METS	WHR METS	
	Relative Humidity	%				
	Barometric Pressure	mbars				
	Rainfall	mm				
	PAR	μmol m ⁻² s ⁻¹				
	Wind Direction	Ø				
	Wind Speed	m s ⁻¹				
Water Presence-Absence	Relative Conductivity	Lux	TAL_STIC	PRF_STIC	WHR_STIC	
(STIC)	Temperature	°C				
	Water Presence-					
	Absence					
Water Level (PRES)	Temperature	°C	TAL_PRES	PRF_PRES	WHR_PRES	
	Barometric Pressure	kPa				
	Water Elevation	masl				
	Water Depth	m				
Outlet Discharge (DISC)	Discharge (Q)	L s ⁻¹	TAL_DISC	PRF_DISC	WHR_DISC	
Outlet Water Quality	Temperature	°C	TAL_EXOS	PRF_EXOS	WHR_EXOS	
(EXOS)	Specific Conductance	μS cm ⁻¹				
	Turbidity	FNU				
	Dissolved Oxygen	mg L ⁻¹				
	fDOM	ppb QSU				
Outlet Absorbance	Turbidity-Compensated A	Absorbance	TAL_SCAN	N/A	N/A	
Fingerprint (SCAN)	Uncompensated Absorbar	nce				

The long-term water quality monitoring sites at each of the study watershed outlets consisted of an EXO2 multiparameter water quality sonde (YSI, Ohio USA) measuring temperature (°C), conductivity and specific conductance (µS cm⁻¹), turbidity (FNU), dissolved oxygen concentration (DO; mg L⁻¹), and fluorescent dissolved organic matter concentration (fDOM; ppb QSU), an installed stilling well and piezometer outfitted with vented pressure transducers to measure changes in surface water and groundwater level, and a pressure transducer deployed in the riparian zone to measure local changes in air



205

210

215

220

225

230

235



temperature and barometric pressure (Fig.1, Table 2). All sensors were set to collect measurements at 15-min intervals throughout the duration of the study. At the outlet of our focal, Piedmont study watershed, we also deployed a spectro::lyser V3 UV-Vis spectrophotometer (s::can, Badger Meter, Milwaukee, Wisconsin USA) to measure light absorbance at wavelengths from 190 to 750 nm at 2.5 nm intervals. Prior to collecting each reading, the EXO and UV-Vis spectrophotometer cleaned the lenses in their optical sensors using an automatic wiper. We conducted regular cleaning and maintenance of all sensors at the watershed outlets every three weeks (sampling approach 1) and recalibrated the EXO water quality sondes every three months (Seybold, 2025).

The seven LTM sites distributed throughout the watersheds were selected to capture a gradient of drainage area accumulation (25%, 50%, and 75%, located on the mainstem of the network), as well as the confluences of two primary tributaries in each network (Fig. 1). At each LTM, co-located stilling wells and subsurface piezometers were installed in the thalweg and instrumented with Onset HOBO U20L pressure transducers (Onset Corporation, Massachusetts, USA) to measure stream water level and vertical head gradients at 15-min intervals. Stilling wells consisted of 2-in diameter PVC installed initially such that the sensor port was within 2 cm of the streambed. In mid-2022, stilling wells were reinstalled such that the sensor port was approx. 10-20 cm below the streambed, but the well was screened above and below the streambed to capture surface water level. Further, piezometers were installed approximately 50 cm below the streambed, with a 20-cm screened interval to capture groundwater level. These locations were maintained every 4-6 months, when sensors were downloaded and relaunched, and physical measurements of water level were taken to ground-truth sensor observations (Zipper et al., 2025a).

The water presence/absence monitoring sites consisted of STIC sensors distributed throughout the watershed to capture a range of topographic conditions. Prior to deployment, STICs were calibrated to ensure good readings in the field (Burke et al., 2024). We utilized a standardized site design (see Zipper et al., 2025b for more information) to select locations randomly across a gradient of drainage area and topographic wetness index (hereafter, TWI; Swenson et al., 2024). At each location, a STIC sensor was placed at the highest longitudinal point in the thalweg of the reach, such that it would capture the first point of network disconnection. The sensor was attached to a ~1-m aluminum U-post using hose clamps, and installed such that the sensor pins were within 1 cm of the stream bed. These sensors were used to measure continuous water presence or absence across the network for the duration of the project. STIC sensors were maintained every 4 months and had their batteries changed every 9 months (Godsey et al., 2024a). Additionally, at every maintenance visit, we collected observations of water presence or absence and recorded the height of sensor pins relative to the bed to account for any sediment accumulation or erosion. Further, in the Piedmont watershed, an additional 29 ("bonus") STIC sensors were deployed for 11 months starting in May 2022 prior to the spatially extensive sampling campaign (see section 2.2.4). We deployed bonus STIC sensors in locations where distances between permanent STIC sensors were large and along more ephemeral channels to increase the spatial resolution of water permanence observations within the existing network and to better capture the network expansion and contraction at maximum extent of the geomorphic channel network (Fig. 1).



240

245

250

255

260



2.2.2 Temporal sampling at the watershed outlet (sampling approach 1)

Between Autumn 2021 and Autumn 2024, we visited the outlet of each watershed every three weeks to assess how flow, hydrologic connectivity, and water quality changed over the course of the study. During these tri-weekly site visits, we conducted regular sensor maintenance, measured hydrologic parameters, and collected water chemistry samples. Hydrologic parameters such as discharge and velocity were only collected if the reach upstream of the outlet sampling site was fully connected and flowing continuously for a distance of at least ten wetted widths. Water samples were only collected if water was present at the outlet (see section 3.3.1). Our temporal outlet sampling data consists of 53, 29, and 44 timepoints for our Piedmont (TAL; Fig. 2B), Appalachian Plateau (PRF; Fig. 3B), and Coastal Plain (WHR, Fig. 4B) watersheds, respectively.

2.2.3 Spatiotemporal sampling across watersheds (sampling approach 2)

To capture variability in watershed-scale hydrologic connectivity, water chemistry, and community dynamics, we conducted three synoptic sampling campaigns at the LTM sites within each study watershed per year for two years. These sets of synoptic campaigns across the three watersheds were aligned with expected seasonal dynamics in flow and connectivity, with a high baseflow campaign occurring in March-May, a dry-down campaign occurring in August, and a wetting-up campaign occurring in January-February. Synoptic campaigns within the same seasonal set were conducted across all three watersheds within 2-3 weeks of each other, with synoptic campaigns within a single watershed taking 1-2 days to complete. During each of these sampling campaigns, we co-collected samples and data for hydrologic (section 3.2), biogeochemical (section 3.3), and microbial community (section 3.4) parameters at the seven LTM sites located throughout each of the study watersheds (including the outlets). Similar to our temporal sampling approaches at the outlet, hydrologic parameters such as discharge were only collected if the reach upstream of the sampling site was flowing, while water chemistry samples were only collected if water was present at the sampling site. Two additional seasonal synoptic sampling campaigns were conducted in January 2022 and November 2023 in our focal Piedmont watershed 1) to test our sampling design and methods and 2) to supplement other ongoing projects in the focal watershed. However, these additional seasonal synoptic campaigns only include limited hydrologic and biogeochemical data products. Lastly, DNA metabarcoding samples for macroinvertebrate community analyses were only collected during the first year of sampling approach 2 campaigns.

2.2.4 Intensive spatial synoptic sampling across Piedmont watershed (sampling approach 3)

We conducted a spatially intensive synoptic sampling campaign from 9-10 June 2022 in the focal Piedmont watershed to capture network-scale patterns and drivers of water persistence, chemistry, and resultant biotic communities. During this sampling campaign, we co-collected samples for biogeochemical parameters (section 3.3) and microbial community analyses (section 3.4) at all permanent STIC, bonus STIC, and LTM sites (including the watershed outlet; n = 50 sites). We only collected samples for biogeochemical parameters and water column microbial community analyses at sites with surface water present at the time of sampling (n = 38 sites). Additionally, we co-collected samples and data for macroinvertebrate community





and hydrologic parameters at a subset of sites (n = 20 sites for hydrologic parameters and n = 28 sites for macroinvertebrate community analyses) as the stream reach lengths required for our field methods for these parameters were longer than actual reach lengths between many of our sites in this campaign (see Section 3.1.2 for hydrologic parameters and Section 3.5 for macroinvertebrate community analyses). We selected this subset of sites to maximize spatial resolution and connectivity variation of our hydrologic and macroinvertebrate community data across the network. To minimize interference and potential contamination, we coordinated our efforts by splitting sampling teams by discipline and sequentially sampled microbial community analyses, biogeochemical parameters, macroinvertebrate community, and hydrologic parameters analyses from downstream to upstream.

3 Methods

275

280

285

290

295

300

3.1 Site characterization

All sensor locations (latitude, longitude) were measured with a eMLID Reach RX multi-band RTK rover with submeter accuracy (eMLID Tech Kft., Hungary). Using these high-resolution sensor locations, we calculated a suite of topographic metrics to contextualize our results: drainage area, distance from outlet, slope, channel slope, slope buffer, and stream slope (Peterson and Jones, 2025a; 2025b; 2025c). First, we obtained 1-m resolution (or finer) DEMs from USGS TNMD v2.0 (https://apps.nationalmap.gov/downloader/) and performed all analyses in R v4.4.0 (R Core Team, 2024). DEMs were processed (filtered, pits filled, depressions breached) using the *whitebox* R package before being cropped to our delineated watershed extent (Wu and Brown 2022). Stream networks were delineated in *whitebox* using thresholds that most closely matched field observations of the geomorphic channel network extent (Piedmont = 10,000 0.92-m cells; Coastal Plain = 12,000 1-m cells; Appalachian Plateau = 60,000 1-m cells). We generated drainage area, distance from outlet, slope, continuous channel slope, and TWI rasters using their respective *whitebox* functions. Drainage area, distance from outlet, slope point, and TWI were extracted from their respective rasters using the high-resolution site locations. Slope buffer was calculated by averaging all raster cells within a 5-m buffer of the locations to integrate local slope. Stream slope was calculated by averaging all continuous channel slope raster cells within the 25-m reach surrounding the location.

3.1.2 Site-level discharge estimates

Between August 2021 and October 2024, we conducted solute-pulse tracer additions of sodium chloride (NaCl) to measure discharge and velocity along the stream reach immediately upstream at each sample site as described in McCleskey et al. (2025) and Godsey et al. (2024b; Table 3). Tracer additions were only conducted if the reach upstream of the sample site was fully connected and flowing continuously for a distance of at least ten wetted widths. During these tracer additions, a known mass of NaCl dissolved in stream water was added instantaneously to the stream while specific conductance (in µS cm⁻¹) was monitored continuously using two conductivity loggers (Solinst) measuring conductivity every 2 s at a downstream monitoring site approximately 10-20 wetted widths from the tracer addition site to ensure complete mixing of the tracer across the stream channel prior to its arrival. We conducted these tracer additions to measure discharge at the watershed outlets every





three weeks during maintenance visits, seasonally at the seven LTM sites, and at n = 20 sites in the focal watershed during the intensive spatial synoptic campaign in June 2022 (Table 1, Fig. 2A, Fig. 3A, Fig. 4A).

Table 3: Summary of field measurements and sample-based water chemistry and dissolved gas data products collected in the Piedmont (TAL), Appalachian Plateau (PRF), and Coastal Plain (WHR) watersheds.

Data Products	Parameter	Units	Data Product Citation Identifier (See Table A1)			
			Piedmont (TAL)	App. Plateau (PRF)	Coastal Plain (WHR)	
Field Measurements (YSIS)	Temperature	°C	TAL_YSIS	PRF_YSIS	WHR_YSIS	
	Conductivity	μS cm ⁻¹				
	Specific Conductance	μS cm ⁻¹				
	Dissolved Oxygen	mg L ⁻¹				
Streamflow (DISL)	Discharge (Q)	L s ⁻¹	TAL_DISL	PRF_DISL	WHR_DISL	
	Velocity (u)	m s ⁻¹	_	_	_	
Water Isotopes (WAIS)	δD	‰	TAL_WAIS	PRF_WAIS	WHR_WAIS	
• • • •	$\delta^{18}\mathrm{O}$	‰	_	_	_	
Seston (TSSS)	TSS	mg L ⁻¹	TAL TSSS	PRF TSSS	WHR_TSSS	
,	sAFDM	mg L ⁻¹	_	_	_	
Nutrients (NUTR)	NH4-N	μg L ⁻¹	TAL NUTR	PRF NUTR	WHR NUTR	
,	$NO_3-N + NO_2-N$	μg L ⁻¹	_	_	_	
	SRP	μg L ⁻¹				
Dissolved Organic Carbon	DOC	mg L ⁻¹	TAL DOCS	PRF DOCS	WHR DOCS	
(DOCS)	200	5 2	1112_2 0 00	114_5000		
Dissolved Organic Matter	Fluorescence at standard peaks	Raman units	TAL DOMS	PRF DOMS	WHR DOMS	
(DOMS)	(A, B, C, M, T)					
	BIX	unitless				
	HIX	unitless				
	FI	unitless				
	Absorbance at 254 nm, 300 nm	m ⁻¹				
	Absorbance slopes (S ₂₇₅₋₂₉₅ ,	nm ⁻¹				
	S ₃₅₀₋₄₀₀ , S ₃₀₀₋₇₀₀)					
	Spectral Slope Ratio	unitless				
	E2:E3	unitless				
Anions (ANIO)	Cl	mg L ⁻¹	TAL ANIO	PRF ANIO	WHR ANIO	
()	Br	mg L ⁻¹				
	F	mg L ⁻¹				
	NO ₃	mg L ⁻¹				
	SO ₄	mg L ⁻¹				
Cations (CAIO)	Ca	mg L ⁻¹	TAL CAIO	PRF CAIO	WHR CAIO	
carions (erno)	Mg	mg L ⁻¹	THE_CHIC	ria_erno	wint_erno	
	Na	mg L ⁻¹				
	В	mg L ⁻¹				
	Si	mg L ⁻¹				
	K	mg L ⁻¹				
	Sr	mg L ⁻¹				
Dissolved Gases (MIMS)	O ₂	5 2	TAL MIMS	PRF MIMS	WHR MIMS	
Jissofved Gases (IVIIIVIS)	Ar		TYF MIINIS	I KI _MIMIS	WIII/_MIMIS	
	N_2					
Greenhouse Gases (GHGS)	$\frac{N_2}{CO_2}$	μМ	TAL GHGS	N/A	N/A	
orcemionse gases (arras)	N_2O	•	TAL_OHOS	1 N/ F1	1 N / <i>F</i> 1	
		μM M				
	CH ₄	μΜ				





310

315

320

325

330

335

340

3.2 Sensor data processing and quality assurance

3.2.1 Water level and rating curves for continuous discharge

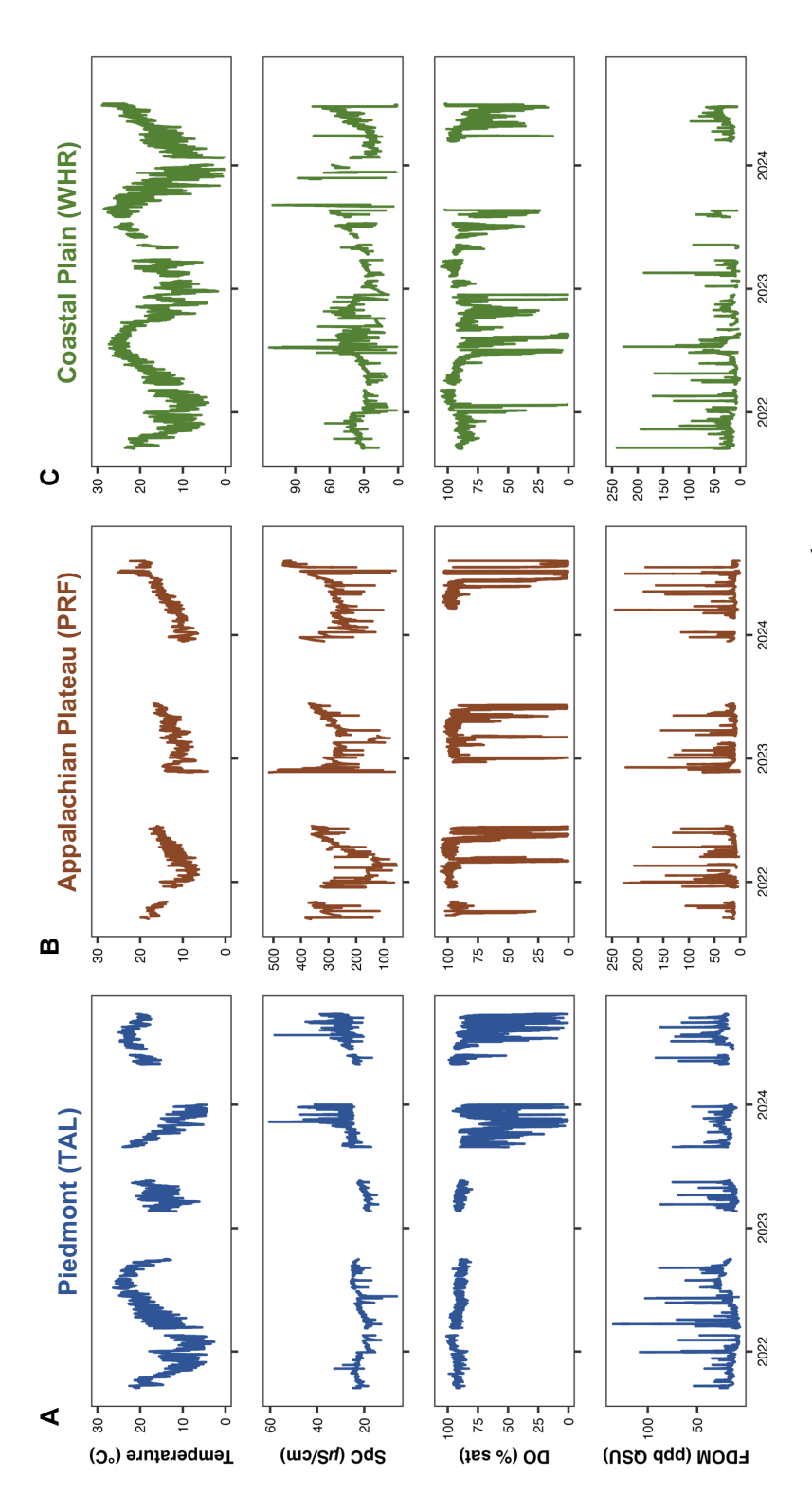
We converted raw sensor data to absolute water level for every stilling well and piezometer. Briefly, raw pressure data from unvented, HOBO U20L sensors (i.e., all LTM sites, and the outlet monitoring stations beginning in 2023) were converted to water pressure using an elevation-corrected, barometric pressure transducer deployed within the study watershed (Table 2, Table A1). This sensor water pressure was converted to water level relative to the sensor-specific datum by correcting for the specific weight of water. Additionally, the outlet monitoring stations were originally instrumented with Seametrics PT12 pressure sensors that recorded relative stream water level (the Piedmont sensor was replaced in January 2023, the Coastal Plain was replaced in June 2023, and the Appalachian Plateau was replaced in June 2024). For all sensors, this relative water level was then converted to absolute water level (waterElevation, masl) using field-observed water level and surveyed elevation data. Further, we calculated water level relative to the average streambed elevation using field observations (waterDepth, m).

Using discharge estimates measured at the outlet of each watershed, we developed site-specific discharge-stage rating curves to estimate discharge at 15-min intervals (Gore and Banning, 2017). This approach allowed us to capture a distribution of flow conditions in each watershed over the three-year study (Fig. 2C, Fig. 3C, Fig. 4C). However, our assessment of stage-discharge relationship during high-flow events is limited by the lack of stormflow discharge estimates. We therefore constrained the upper limit of our stage-discharge rating curves to stage measurements less than bankfull stage estimated from on-site topographic surveying and flagged discharge measurements greater than 200% of our highest measured discharge estimates at a given site.

3.2.2 Water presence-absence

We deployed at least 20 STIC sensors in each of our three watersheds to measure water presence or absence continuously throughout the network. These sensors, modified following Chapin et al (2014) from a HOBO Pendant logger, recorded temperature and relative conductivity (in lux) at 15-min intervals. Then, using a project-wide reproducible workflow outlined in Zipper et al. (2025b), we converted relative conductivity to binary water presence or absence based on sensor-specific thresholds identified through laboratory calibrations (Fig. 2A, Fig. 3A, Fig. 4A). These water presence/absence observations were then compared to field observations, quality-checked, and flagged based on data quality. To capture expansion and contraction dynamics in each stream network, we used data from all permanent STIC sensors within each watershed to estimate the percent of active network wet at each timepoint as the number of wet STIC sensors normalized for the total number of STIC sensors (Fig. 2D, Fig. 3D, Fig. 4D). Prior to calculating percent network wet for each watershed, we removed STIC sensors where > 50% of measurements received a poor data quality flag over the study period (n = 0 sensors for TAL, n = 1 for PRF, n = 6 for WHR), estimated daily wet/dry conditions at each site as the daily mode of each 15-min STIC time series, and interpolated data gaps for up to two days using the STIC.RFimpute() function in the *StreamDAG* R package (Aho et al., 2023).





gaps in time series are due to either dry conditions, burial, sensor malfunction, or sensor maintenance, each of which are flagged in saturation; third row), and fluorescent dissolved organic matter (FDOM; ppb QSU; fourth row) at the watershed outlet over the Figure 5: Time series of temperature (°C; first row), specific conductance (SpC; μS cm⁻¹; second row), dissolved oxygen (DO; % FDOM concentrations are compensated for temperature and turbidity effects following methods outlined in section 3.2.3. Data deployment period in the Piedmont (TAL; A), Appalachian Plateau (PRF; B), and Coastal Plain (WHR; C) study watersheds. the published data sets.



350

355

360

365

375



345 3.2.3 Multi-parameter water quality sondes

Prior to any parameter-specific corrections or analyses, we used a standardized protocol to check and assure the quality of our high-frequency water quality data collected using the EXO2 multiparameter sondes deployed at each of our watershed outlets (Fig. 5). We first identified and filtered out unrealistic values in each of the temperature, conductivity, specific conductance, dissolved oxygen concentration, and turbidity time series using 1) an alpha filter to remove erroneous values (e.g., error code readings, negative concentrations) and 2) a conservative beta filter that removed measurements that were greater than three standard deviations of a rolling mean or greater than three moving absolute deviations. We then manually checked and flagged any remaining time periods of instrument malfunction, burial, and desiccation using field notes, water level data collected from the co-located stilling well, and sudden baseline shifts in the conductivity and turbidity data from the watershed outlet. We removed data during periods of burial, desiccation, and sensor malfunction corroborated by field notes and observation (Fig. 5). Using the pre- and post-calibration values, we determined that the influence of sensor drift between calibrations (every three months) was negligible for sensor-derived water quality data (< 5% difference).

We corrected fDOM measurements for both instrument- and site-specific effects of temperature as well as suspended and dissolved particles that can influence the attenuation of light in water (Fig. 5). Briefly, we used methods described in Watras et al. (2011) and the EXO User Manual (2020) to compensate raw fDOM measurements for temperature effects on fluorescent intensity using a reference temperature of 25 °C and a specific temperature attenuation coefficient of -0.01 °C⁻¹. We tested for potential filtering effects due to dissolved particles in the water, or the inner filter effect, and suspended particles following laboratory methods described in Downing et al. (2012). We determined that inner filter effects likely played a negligible role in influencing fluorescence intensity measurements at our sites given consistently low absorbance values in site-specific filtered water, even when turbidity exceeded 1000 FNU, and decided not to include inner filter-effect fDOM corrections. We corrected for the influence of suspended particles, assessed as turbidity, on fDOM measurements following methods adopted from Downing et al. (2012) and Senatore et al. (2023). We estimated the turbidity attenuation factor for each fDOM sensor by first calculating the ratio of temperature-compensated fDOM measurements and measured dissolved organic carbon (DOC) concentrations from grab samples (fDOM/DOC) and fitting an exponential decay function to each fDOM/DOC vs. turbidity relationship, following expected trends of the Beer-Lambert Law. To derive these turbidity attenuation factors, we used paired fDOM, DOC, and turbidity measurements from samples collected in the field throughout the sensor deployment, as well as DOC samples and fDOM readings collected during laboratory tests in which we systematically increased turbidity to the highest recorded turbidity values from each site (~1000 FNU) to simulate the highest flow-induced turbidity conditions in our deployment (Fig. 5). These turbidity attenuation factors were comparable to those reported by others in previous work using similar laboratory-correction procedures (Downing et al., 2012; Senatore et al., 2023).

3.2.4 UV-Vis absorbance fingerprint

Due to the complexity of the absorbance spectra time series generated by the submersible UV-Vis spectrophotometer (s::can spectro::lyser V3), we used a simplified version of our data quality-assurance methods for sensor-derived water



380

385

390

395

400

405

410



chemistry to filter out erroneous absorbance spectra. We used error codes recorded on the instrument, field notes, and water-level and turbidity data from the watershed outlet to help remove all spectra during periods of instrument malfunction, burial, and desiccation. We further filtered the absorbance data time series by first selecting three wavelengths (200 nm, 255 nm, 400 nm) to be representative of the entire UV-Vis absorbance spectra. We removed entire recorded spectra when 1) absorbance values at a given time point were negative at 200 or 255 nm and 2) when absorbance values at a given time point exceeded three standard deviations of the rolling mean absorbance values at 200, 255, or 400 nm. We processed and opted to publish both the turbidity-compensated and uncompensated absorbance spectra time series for the entire deployment record (Table 2).

3.3 Water chemistry sampling and analysis

3.3.1 Sample collection

We collected surface water samples following standard operating procedures outlined by the "Aquatic Intermittency effects on Microbiomes in Streams" project (Burgin, 2024). During each sampling event, we collected water samples for dissolved organic carbon (DOC), nutrients including ammonium (NH₄-N), nitrate/nitrite (NO₃-N + NO₂-N), and soluble reactive phosphorus (SRP), anion (including NO₃, Cl, SO₄), and cation (including Ca, Na, K, Mg, Si) concentrations, as well as water isotopes (δD , $\delta^{18}O$), dissolved organic matter (DOM) optical properties, total suspended solids (TSS), and seston ashfree dry mass (sAFDM) at a given site (Table 3, Table A1). We filtered DOC samples through pre-ashed 0.7-um glass fiber filters (Whatman GF/F) into triple-rinsed 60-mL amber high-density polyethylene (HDPE) bottles, acidified DOC samples to a pH of 2 using concentrated HCl, and refrigerated samples at 4 °C for up to 28 days prior to analysis. We filtered samples for nutrient, anion, and cation concentrations through sterile, 0.45-um PVDF filter cartridges (VWR) into triple-rinsed 50-mL sterile centrifuge tubes for nutrients and 30-mL clear HDPE bottles for anions and cations, respectively. We kept nutrient and anion samples frozen and acidified cation samples to a pH of 2 using concentrated HNO3, which were kept refrigerated at 4° C until analysis. We collected samples for water isotopes by triple-rinsing and filling clear borosilicate sample bottles with conical caps underwater until no headspace remained in the sample to reduce potential evaporative fractionation. We then sealed caps of each water isotope sample with parafilm and stored at room temperature until analysis. For DOM samples, we filtered water through 0.22-um cellulose acetate filters into triple-rinsed 30-mL amber HDPE bottles until no headspace remained and then refrigerated until analysis. We collected triplicate samples for all surface water chemistry except for water isotopes, which we collected in duplicate. To measure TSS and sAFDM concentrations, we collected 2-3 replicates of unfiltered stream water in clean 1-L Nalgene bottles after triple-rinsing in the field, which were then stored on ice and brought to the lab for filtering. We vacuum-filtered known volumes of stream water within 24 hours onto pre-ashed and pre-weighed 0.7-µm glass fiber filters (Whatman GF/F), placed in a drying oven at 50 °C for at least 48 hours, and then weighed for the sample dry mass. We calculated TSS concentration (in mg L-1) as the sample dry mass normalized for the volume of water filtered. To determine sAFDM concentrations, we ashed the dried sample filters at 500 °C for four hours, re-wet with Type 1 water, dried at 50 °C for at least 48 hours, and weighed for the remaining sample mass. We calculated seston AFDM concentration (in mg L⁻¹) as the difference in dry mass before and after ashing normalized for the volume of water filtered.



415

420

425

430

435



3.3.2 Dissolved water chemistry analysis (NUTR, ANIO, CAIO, DOCS)

After field sampling, samples were allowed to come to room temperature prior to analyses. We briefly describe water chemistry analysis below. Further details of instrument specifics and parameters for all analyses can be found in the metadata descriptions provided with each specific data publication in the AIMS Hydroshare repository (Table 3, Table A1). We analyzed stream water samples for nutrient concentrations using an AQ300 Discrete Analyzer (SEAL Analytical, Mequon, Wisconsin, USA). Briefly, we analyzed samples for soluble reactive phosphorus (SRP; µg L-1) ammonium (NH4-N; µg L-1), and nitrate/nitrite (NO₃-N + NO₂-N: μg L⁻¹) using the ascorbic acid method (SRP detection limit = 6 μg L⁻¹; Murphy and Riley, 1962), phenol-hypochlorite method (NH₄-N detection limit = 11 μg L⁻¹; Solórzano, 1969), and cadmium reduction method (NO₃-N detection limit = 11 μg L⁻¹; APHA, 2017), respectively. While all water samples collected for nutrient determination were analyzed for SRP and NH₄-N, only samples collected before July 2024 were analyzed for NO₃-N using the cadmium reduction method. Aqueous concentrations of anions (fluoride [F], chloride [Cl], bromide [Br], nitrate [NO₃], and sulfate [SO₄]) were determined using ion chromatography with either an IC-3000 IC system (Dionex, Sunnyvale, CA) with a Dionex IonPac AS15 column (2 mm by 50 mm, Thermo Scientific) for samples collected prior to January 2023 or a Metrohm 930 Compact IC Flex (Metrohm, Riverview, Florida) for samples collected after January 2023. We confirmed that anion concentrations were comparable between these two instruments within the range of standard error estimates typical of each analyte by running sets of paired water samples on each instrument. We also found that nitrate concentrations (in µg NO₃-N L⁻¹) were comparable between samples analyzed via cadmium reduction and via ion chromatography. Aqueous concentrations of base cations (sodium [Na], calcium [Ca], boron [B], magnesium [Mg], silicon [Si], potassium [K], and strontium [Sr]) were determined via inductively coupled plasma-atomic emission spectrometry (ICP-AES) using a Horiba Ultima 2 fitted with an AS 500 autosampler (Horiba Jobin Yvon). Samples for base cation determination were re-filtered using a 0.2-µm PES filter immediately prior to analysis. Dissolved organic carbon concentrations were determined as non-purgeable organic carbon (in mg L⁻¹) via acid-catalyzed, high-temperature combustion using a Shimadzu TOC-V total organic carbon analyzer (Shimadzu Scientific Instruments, Kyoto, Japan).

3.3.3 Dissolved organic matter characterization (DOMS)

Excitation-emissions matrices and absorbance spectra were collected for DOM characterization on a Horiba Aqualog from 249 to 830 nm at 5-nm increments at the University of Alabama and/or Idaho State University. Integration times varied from 2 to 4 s, based on sample concentration. EEMs were blank-corrected, Raleigh masked, inner filter effects were removed, and values were Raman-normalized using Aqualog software. Standard fluorescence metrics were calculated from corrected EEMs using the *StaRdom* package (Pucher et al., 2019) in R (Table 3, Table A1). These included: biological index (BIX; an indicator of autotrophic DOM; Fellman et al., 2010), fluorescence index (FI; an indicator of relative terrestrial or microbial source of organic matter; McKnight et al., 2001), and humification index (HIX, an indicator of the extent of humification;





Ohno, 2002). We also calculated fluorescence at standard peaks: amino acid-like peak tyrosine (B) and amino acid-like peak tryptophan (T), which both indicate labile protein-like DOM; humic-like peaks A and C, which both indicate DOM derived from terrestrial vascular plants, aromatic, likely higher-molecular weight DOM; and humic-like peak M (M), which is considered less aromatic and lower molecular weight than peaks A and C (Coble, 1996; Fellman et al., 2010).

Absorbance metrics were also calculated in *StaRdom* (Table 3, Table A1), including absorbance at 254 nm (a254; which is correlated with aromaticity; Weishaar et al., 2003), absorbance at 300 nm (a300; a proxy for photosensitive, chromophoric DOM; Clark et al., 2019) and E2:E3 (the ratio of absorbance at 250 nm to absorbance at 365 nm), which is negatively correlated with molecular weight and aromaticity (Li and Hur, 2017). We calculated absorbance slopes from 275-295 nm (S27_5295), 350-400 nm (S350_400), and 300-700 nm (S300_700), which are all proxies for DOM molecular weight (Helms et al. 2008), slope ratio (SR; the ratio of the best-fit slopes of absorbance from 275-295 nm to the slope of absorbance from 250-400 nm) which is negatively correlated with molecular weight and sensitive to photobleaching (Helms et al., 2008).

3.3.4 Water isotope analysis (WAIS)

All water isotope samples were stored in darkness at room temperature until analysis. The first sample from each duplicate pair was designated for analysis, while the second served as an archive. Oxygen and hydrogen isotope ratios (δ¹⁸O and δD) were measured using a cavity ring-down spectroscopic isotope water analyzer (Picarro L2130-i, Picarro Inc., CA). For each sample, six sequential sub-samples were analyzed to account for memory effects. The first three sub-samples equilibrated the measurement cavity, while the final three sub-samples were used to calculate δ¹⁸O and δD ratios. To correct for instrument drift and ensure measurement precision, all samples were calibrated against internal secondary standards. The internal secondary standards were previously calibrated against International Atomic Energy Agency (IAEA) primary standards referenced to Vienna Standard Mean Ocean Water. All isotope values are reported as per mil (‰) deviations relative to VSMOW.

3.4 Dissolved gas sampling and analysis

470 3.4.1 Sample collection

Dissolved gas sampling of dinitrogen (N₂), oxygen (O₂), and argon (Ar) as well as greenhouse gases (GHGs; carbon dioxide [CO₂], methane [CH₄], and nitrous oxide [N₂O]) took place during both sampling approaches 2 and 3 (Zarek and Burgin, 2024; Burgin et al., 2025). For sampling approach 2, we collected samples for N₂, O₂, and Ar at the seven LTM sites in all three watersheds while GHG samples were only collected in the Piedmont watershed. For sampling approach 3, samples for N₂, O₂, and Ar as well as GHGs were collected at 40 locations throughout the Piedmont watershed. For N₂, O₂, and Ar sampling, we used one 140-mL syringe with a two-way stopcock and long tubing extender attached on the end of the stopcock to collect a bubble-free water sample from the stream. Upon sample collection, we expelled 40 mL of water through the long tubing extender into three 12-mL vials (Exetainer*, Labco, UK). In each vial, we overflowed the sample vial volume ~3x



480

485

490

495

500

505

510



before forming a meniscus and then preserving with 0.2 mL of 50% ZnCl₂. Samples were capped, inverted to make sure there were no bubbles, and stored underwater in a container and on ice until we returned to the lab (Zarek and Burgin, 2024). GHG samples were collected using a headspace equilibrium technique (Burgin et al., 2025). Using a 60-mL syringe, we pulled 20 mL of a bubble-free surface water sample from the stream, and we pulled a 10-mL argon headspace into a 30-mL syringe. Then under water, we transferred the known volume of argon to the known volume of surface water and shook the syringe vigorously for 5 min to equilibrate the dissolved gases in the water with argon. After 5 min, 10-12 mL of headspace from each syringe was transferred to a 6-mL pre-evacuated vial (Exetainer*, Labco, UK). All GHG samples were collected in triplicate and stored in a container until we returned to the laboratory.

3.4.2 Dissolved gas analysis (MIMS, GHGS)

Samples for CO₂, CH₄, and N₂O (GHG) were analyzed via a gas chromatograph equipped with a flame ionization detector and electron capture detector (Agilent7890B, Santa Clara, CA). We calculated GHG concentrations using Henry's Law and the Ideal Gas Law constants (Weiss, 1974; Weiss and Price, 1980; Wiesenburg and Guinasso, 1979; Table 3, Table A1). N₂, O₂, and Ar were measured via a membrane inlet mass spectrometer (MIMS). The concentrations of N₂, Ar, and O₂ were determined using the *mimsy* R package which calculates gas concentrations for MIMS samples based on known solubility conditions, including barometric pressure, specific temperature, and salinity (Kelly, 2020; Table 3, Table A1).

3.5 Microbial community collection and analysis

3.5.1 Field site characterization and sample collection

Sampling of microbial DNA, extracellular enzyme activity (EEA), chlorophyll-*a* (Chl-*a*), and habitat-specific ashfree dry mass (AFDM) took place during the approach 2 and approach 3 sampling events according to the AIMS microbial field sampling protocol (Zeglin and Busch, 2024; Table 1) and are consistent with methods described in Bond *et al.* (2025). Briefly, for each sampling event at each site, composite samples for microbial analyses were collected for each of four microbial habitat compartments (sample types): decaying leaf litter, rock surfaces (epilithon), benthic sediments, and surface water (Table 4). For each event at each site, composite samples of each sample type were subsampled for DNA, EEA, and AFDM. Subsamples for Chl-*a* were collected for surface water and rock surfaces. In the field, DNA subsamples were flashfrozen and stored in liquid nitrogen and then transferred to a -80 °C freezer for storage in the lab, while EEA, AFDM, and Chl-*a* samples were placed on dry ice in the field and -20 °C for storage in the lab. Further details on sample collection and site characterization are as follows.

Consistent with the methods described in Bond et al. (2025), the sampling area at each site was defined as a 1-m long section of the stream centered on the in-stream sensor for each site and spanning the full wetted width of the stream. For the outlet sites in each watershed, where the sensors were in pools too deep to sample, sampling took place in a shallower transect immediately adjacent to the sensor pool. Sampling areas for dry sites were determined based on visual indicators of past water



525



level. Sampling areas were subdivided into three sub-areas of equal width, and equal parts of each sample type were collected and combined from each sub-area to make composite samples for each sample type.

Table 4: Summary of microbial and macroinvertebrate community data products collected in the Piedmont (TAL), Appalachian Plateau (PRF), and Coastal Plain (WHR) watersheds.

Data Product	Parameter	Habitat				Data Product Citation Identifier (See Table A1)		
		Water Column	Sediment	Leaf	Epilithic Biofilm	Piedmont (TAL)	App. Plateau (PRF)	Coastal Plain (WHR)
Microbial and Macroinvertebrate Field Metadata (MIME, MAME, AFDM, CHLA)	Wetted width (m) Sediment Texture Percent Rocks Percent Leaf Litter Percent Sediment Leaf Species AFDM Chlorophyll a	x x	X	x	x x	SE_MIME, TAL_MAME, SE_AFDM, SE_CHLA	SE_MIME, PRF_MAME, SE_AFDM, SE_CHLA	SE_MIME, WHR_MAME, SE_AFDM, SE_CHLA
Macroinvertebrate Metabarcoding (MACR)	Species list					SE_MACR	SE_MACR	SE_MACR
Microbiome	16S (bacteria, archaea) ITS (fungi)	Х	X X	X X	X X	*See Table A3 for NCBI SRA BioProject Accession Numbers		roject Accession
Extracellular Enzyme Activities (EEAS)	β-Glucosidase Phenol Oxidase Peroxidase	X	X X X	x x x	Х	TAL_EEAS_A2, TAL_EEAS_A3	PRF_EEAS	WHR_EEAS
	Phosphatase N-Acetylglucosaminidase	X X	X X	X X	X X			

Water was collected first to prevent benthic disturbance from contaminating the sample. Using a sterile 60-mL syringe, 120 mL of surface water was collected from each of the three sub-areas and combined in a 500-mL Nalgene bottle. The composite water sample was subsampled for DNA by filtering up to 120 mL (or until the filter clogged) onto a sterile 0.22-µm cellulose acetate filter, and up to 60 mL each were filtered onto GF/F filters for Chl-a and water column AFDM. For epilithic biofilms, one rock was collected from each sub-area, scraped using a sterile wire brush over a 25-cm² surface area on the top of each rock, and rinsed into a sterile plastic container using 50 mL of sterile deionized water. In cases where 25-cm² surface area could not be sampled, we collected a trace of the rock and estimated surface area using ImageJ. The resulting slurry was mixed and subsampled, with up to 10 mL of slurry (lower if filter clogged) collected for DNA on a 0.22-µm cellulose acetate filter and up to 10 mL each on GF/F filters for epilithic AFDM and Chl-a. For leaf litter samples, one decaying leaf was collected from each of the three sub-areas, identified to the lowest taxonomic level possible and cut in half, and leaf halves from each sub-area were combined for one composite leaf litter sample for DNA and one composite leaf litter sample for EEA and AFDM. For sediment samples, a 2-cm core of sediment was collected from each sub-area, and all three were combined



535

540

545

550

555

560



into a 50-mL centrifuge tube and mixed by shaking for 60 s. At least 5 mL of the mixed sediment was transferred to a sterile 15-mL tube for DNA, and the remaining material was collected for EEA and sediment AFDM in a sterile 50-mL tube.

3.5.2 Chlorophyll a and ash-free dry mass of leaf litter, sediment, water column, and epilithon

For water and epilithon samples, Chl-*a* was extracted from the GF/F filters in 90% ethanol (2 mL for water filters and 5 mL for epilithon filters) at 80 °C for 5 min, steeped overnight at 4 °C in darkness, and quantified the following day using a Shimadzu 10ADvp series high-performance liquid chromatography equipped with a Shimadzu RF10Axl fluorescence detector (excitation 430nm, emission 670 nm; Meyns et al., 1994). Chl-*a* content was calculated as μg L⁻¹ for water samples and as μg cm² for epilithon samples (Table 4, Table A1). Filters for water column and epilithon AFDM quantification were initially dried at 55 °C for at least 48 h, weighed, combusted at 500 °C for 2 h, and reweighed. For leaf litter and sediment AFDM, we recorded the initial wet mass of each subsample prior to drying at 70 °C for 48 h, after which they were reweighed to obtain dry mass. These dried subsamples were then combusted at 500 °C for 2 hours and reweighed. Habitat-specific AFDM (water column, epilithon, leaf litter, sediment) was calculated as the difference between dry mass and ash mass for each subsample and expressed as the proportion of AFDM relative to total dry mass for each sample (Table 4, Table A1). Concentration of AFDM (mg mL⁻¹) was also calculated surface water, and the areal AFDM (mg cm⁻²) was calculated for rock surfaces.

3.5.3 DNA extraction and metabarcoding

DNA extraction followed the same methods as in Bond et al. (2025). Briefly, DNeasy PowerSoil® Pro Kits (Qiagen, Germany) were used following a modified version of the manufacturer's protocol. For water and epilithon samples, sample filters were cut in half, with one half used for DNA extraction and the other half archived at -80 °C. For leaf litter and sediments, samples were briefly defrosted, homogenized using a sterile scoopula, and a known wet mass of material was used for DNA extraction while the remaining material was archived at -80 °C. DNA extraction then proceeded for all sample types following the standard Qiagen DNeasy PowerSoil Pro Kit Handbook, but with the addition of a second elution step with a 5-min incubation to increase DNA recovery. Nucleic acid yield was measured using the NanoDrop OneC (Thermo Scientific, Wilmington, Delaware, USA).

Aliquots of extracted DNA were shipped on dry ice to Idaho State University (ISU) for 16S library preparation, retained at University of Southern Mississippi (USM) for ITS library preparation, and stored at -80 °C at both locations. The community metabarcoding approach for fungi (ITS rDNA) is described in Bond et al. (2025); for prokaryotes (16S V4), the approach was based on the Earth Microbiome Project (Thompson et al., 2017). Briefly, for fungi, the ITS1 rDNA region was targeted using the forward primer BITS (5'ACCTGCGGARGGATCA-3') and the reverse primer B58S3 (5'GAGATCCRTTGYTRAAAGTT-3') (Bokulich and Mills, 2013), with primers given unique 8-nt barcodes for a dual index barcoding approach (Kozich et al., 2013). PCR amplifications took place in 20-μL reactions with 17 μL AccuPrime Pfx Supermix (Invitrogen/ThermoFisher, Carlsbad, CA, USA), 5 pmol of each primer (1 μL each), and 1 μL of DNA template,



565

570

575

585

590

595



with a final template concentration <4 ng μL⁻¹ per reaction. Thermal cycler conditions were identical to those in Bond et al. (2025): denaturation at 95 °C for 2 min and then 35 cycles of 95 °C for 30 s, 55 °C for 30 s, and 72 °C for 60 s, with a final extension at 72 °C for 5 min. ITS library clean-up and normalization used the SequalPrep Normalization Plate Kit (Applied Biosystems/ThermoFisher, Foster City, CA, USA) and sequencing was performed on the Illumina MiSeq platform (Illumina Inc., San Diego, CA, USA) at the University of Maryland Institute for Genomic Sciences (UMD IGS).

For bacteria and archaea, the 16S V4 region was targeted using barcoded forward 515F primer (5'-3': GTGYCAGCMGCCGCGGTAA) (Parada et al. 2016), and barcoded reverse 806R primer (5'-3': GGACTACNVGGGTWTCTAAT) (Apprill et al. 2015). PCR amplifications took place in 25-μL reactions consisting of 12 μL Invitrogen Platinum Hot Start PCR 2X Master Mix (Catalog Number 13000013, Thermo Fisher Scientific), 0.2 μM of each primer, 2-5 μL template DNA, and the remaining volume was nuclease-free water (You et al. 2023). Thermal cycler conditions were: 94 °C for 3 min, followed by 35 cycles of 94 °C for 45 s, 50 °C for 60 s, and 72 °C for 90 s, and a final extension at 72 °C for 10 min. 16S library clean-up used the MagBio HighPrep PCR Clean-up System (Catalog Number AC-60050, Illumina) following the Illumina PCR Clean-up 2 Protocol (Illumina 16S Metagenomic Sequencing Library Preparation). Sequencing was done at the Molecular Research Core Facility at Idaho State University using the Illumina MiSeq platform (San Diego, CA) following the manufacturer's protocols.

3.5.4 Extracellular enzyme activity

Extracellular enzyme activities involved in the degradation of plant-derived organic matter — β -glucosidase, phenol oxidase, and peroxidase — as well as enzymes associated with phosphorus (phosphatase) and nitrogen (N-acetylglucosaminidase) mineralization were measured following the protocols of Jackson et al. (2013, 2006).

For water and epilithon samples, the activities of β -glucosidase, phosphatase, and N-acetylglucosaminidase were determined using 4-methylumbelliferone (MUB)-linked fluorogenic substrates. Each assay consisted of 200 μ L of sample (thawed, vortexed) dispensed into eight replicate wells per enzyme (Table A2). To each well, 50 μ L of 5 mM bicarbonate buffer, 50 μ L of 10 μ M MUB standard, and 50 μ L of the appropriate substrate solution were added in sequence, with controls and standards prepared as described in Jackson et al. (2013). Fluorescence was measured every 5 min over a 30-min period using a BioTek Synergy 2 microplate reader (BioTek Instruments, Winooski, VT) with excitation at 350 nm and emission at 450 nm. Enzyme activity was calculated as the rate of substrate conversion and expressed as μ mol h^{-1} L⁻¹ for water and μ mol h^{-1} cm⁻² for epilithon (Table 4, Table A1).

For leaf litter and sediment, enzyme activities were assayed using colorimetric 4-nitrophenyl (pNP)-linked substrates for hydrolases and 3,4-dihydroxyphenylalanine (L-DOPA) for oxidases (Table A2). Slurries were prepared from a known wet mass of material, and 150 μ L of slurry was added to each well of a 96-well deep-well block. For each replicate, 150 μ L of substrate solution was added; substrate controls received the same volume of substrate, and sample controls received sterile water. Peroxidase assays included an additional 15 μ L of 0.3% H_2O_2 per well. Incubation times were 1 h (phosphatase and β -glucosidase), 2 h (oxidases), and 3 h (N-acetylglucosaminidase) at room temperature. Following incubation, plates were



600

605

610

615

620

625



centrifuged at $4000 \times g$ for 5 min, and 150 μ L of supernatant was transferred to clear microplates containing 150 μ L of either 1 M NaOH for pNP assays or water for L-DOPA assays. Absorbance was measured at 410 nm for pNP-linked substrates and 460 nm for L-DOPA. We report all enzyme activities, including water and epilithon samples, both in units of μ mol h^{-1} g^{-1} habitat-specific dry weight (DW) and μ mol h^{-1} g^{-1} habitat-specific AFDM (Table 4, Table A1).

3.6 Macroinvertebrate community collection and analysis

3.6.1 Field site characterization and sample collection

We collected benthic macroinvertebrate samples during Approach 1, 2 (only for the Piedmont and Coastal Plains watersheds), and 3 sampling events following standard operating procedures outlined by the "Aquatic Intermittency effects on Microbiomes in Streams" project (Allen, 2024). We delineated a 100-m reach at each sensor location by measuring 50 m upstream and downstream from the sensor. We collected Surber samples (0.09 m², 500-µm mesh) every 20 m beginning at the most downstream location for a total of six samples within each reach. If sites were not conducive to Surber sampling, we used alternatives such as a D-net, taking care to disturb a similar area (all sampler types were noted). These samples were then combined to create one sample per sensor reach by removing any large material, such as leaves or sticks, and elutriating before preserving in 95% ethanol. We stored samples on ice before returning to the lab where ethanol was refreshed and samples frozen at -20 °C. Additionally, we recorded habitat data at each sampling location within the 100-m reach including wetted width (m), substrate composition (percent coverage based on size scale), percent filamentous algal cover, percent epilithic algal cover, canopy cover upstream and downstream, habitat type (e.g., riffle, run, pool), and whether wet or dry. We also noted whether the reach was flowing or disconnected (Table 4, Table A1).

3.6.2 Metabarcoding methods

We contracted a commercial laboratory (Jonah Ventures, Boulder, CO) to process and sequence macroinvertebrate samples using primers BE and F230 from the CO1 gene (CO1 F230 fragment: (Hajibabaei et al., 2012); CO1 BE fragment: (Gibson et al., 2015). Briefly, the commercial laboratory homogenized community samples using a handheld immersion blender, extracted DNA with a Qiagen DNeasy PowerSoil Pro Kit (as in microbial DNA extraction above), then amplified samples using the above primers. They conducted PCRs with initial denaturation at 95 °C for 5 min, followed by 40 cycles of 40 s at 95 °C, 1 min at 46 °C, 30 s at 72 °C, and a final elongation at 72 °C for 10 min. Samples were then cleaned using *Exo1/SAP*, and pooled, normalized and indexed. Jonah Ventures then sent samples for sequencing at the CU Boulder BioFrontiers Sequencing Center, where the Center used the v2 500-cycle kit with appropriate quality-control measures. Jonah Ventures then demultiplexed sequenced samples using *phigs* v2.1.0 followed by removal of gene primers and merging read pairs. They then clustered read pairs using *unoise3* denoising algorithm in vsearch (Rognes et al., 2016). Sequences with less than 8 reads were discarded. Taxonomy was assigned using a custom best-hits algorithm with reference to NCBI Gen Bank to each Exact Sequence Variant (ESV).





630

635

640

645

650

655

660

4 Data Management / Availability

At the beginning of the project, we developed standard operating procedures (SOPs) to ensure that fieldwork methods would be the same across every watershed in the project. In addition, all datasets produced by the project contain the same metadata and are in the same format to promote interoperability. Hydrologic sensor data are published as one file for every sensor for every year; where multiple sensor datasets of the same type of data were collected within a watershed, separate files were generated for each sensor by site or sublocation within a site (e.g., time series data for each surface water and groundwater sensor across the seven long-term monitoring sites in a watershed are published as separate files in the same resource). Alternatively, water quality sensor data (i.e., EXOS, SCAN) are published as a single time series for the entire period of its respective data collection. Additionally, sample-based datasets of a given type are published separately for each watershed, but collated across sampling approaches whenever applicable (e.g., all Piedmont nutrient data for sampling approaches 1, 2, and 3 are in one dataset). For each dataset, data collected based on different sampling approaches are designated using approach-specific binary operator columns. This method also applies to the microbial and macroinvertebrate data, with data across approaches combined into a single file for the full project.

All SOPs, sensor-based datasets, hydrologic and water chemistry datasets, and descriptive datasets such as watershed characteristics and environmental parameters are deposited in the HydroShare data repository, operated by the Consortium of Universities for the Advancement of Hydrologic Science, Inc. (CUAHSI; https://www.hydroshare.org/group/247). However, raw sequence data produced by microbiome analyses were posted in the National Center for Biotechnology Information Sequence Read Archive (NCBI SRA). All Illumina reads from 16S rRNA gene sequencing are deposited under the BioProject accession numbers PRJNA1288562 and PRJNA1289217 (Table A3). Illumina reads from ITS sequencing are deposited under the BioProject accession number: PRJNA1288519, PRJNA1289149, and PRJNA1289189 (Table A3). As per HydroShare standards, each published dataset is given a unique citation and digital object identifier. Due to the large number of datasets with unique citations and digital object identifiers (n = 61 unique datasets published to Hydroshare, n = 5 unique datasets published to NCBI), we chose to include specific datasets throughout the manuscript when only when relevant and included full citations all datasets in Table A1. Each citation in Table A1 is linked with a specific data citation product identifier, which are used to link dataset citations to summary information provided in Tables 2-4.

5 Conclusions

We provide detailed temporal and spatial hydrologic, biogeochemical, microbial, and aquatic insect data for three non-perennial streams in the southeastern USA, contributing novel datasets that are rarely collected in unison. In addition, while non-perennial streams have gained attention in recent years, these ecosystems are rarely studied in mesic areas, despite their global prevalence. This data compilation is part of a larger, cross-continental study of aquatic intermittency effects on microbiomes in streams (i.e., AIMS) with comparable watershed studies in different climatic regions across the USA. By co-

https://doi.org/10.5194/essd-2025-559
Preprint. Discussion started: 23 October 2025

© Author(s) 2025. CC BY 4.0 License.



665

675



collecting data through a large, interdisciplinary project across different spatial and temporal scales we will better understand how physical and biological drivers interact to impact water quality in watersheds with non-perennial reaches. As the climate continues to change globally, more perennial rivers are expected to become intermittent, and understanding how water quality and riverine communities respond through space and across time to variations in flow will be vital to the conservation of freshwater resources.

6 Author Contributions

All co-authors participated in the field collection, laboratory analyses, data processing and quality assurance, and/or curation of individual data products. SP was primarily responsible for writing the initial and final draft of this manuscript with assistance from DMP, CRS, CTB, ALKT, RLH, and CNJ. SP, DMP, CRS, MHB, CTB, ALKT, RLH, and KZ assembled and published individual data products to repositories. All co-authors, particularly DMP, CRS, MAW, KZ, MHB, SLS, and JPB, contributed to editing and reviewing manuscript drafts.

7 Competing Interests

The authors declare no conflicts of interest or competing interests.

8 Acknowledgements

This work was supported financially by the National Science Foundation Office of Integrative Activities (OIA Award #2019603). We gratefully acknowledge the US Forest Service, the Weyerhaeuser Company, and private landowner John Gully for their logistical support, management and access to the research watersheds. We would also like to thank Dr. Jami Nettles, Dr. Dawn Lemke, Helen Czech, Patience Knight, Lidia Molina Serpas, Justus King, Caroline Anscombe, Jacob Ackerman, Zacharie Loveless, Masi Veisi, and Claudia Dorantes-Perez and many other friends and colleagues for their help with instrument maintenance, fieldwork, laboratory analyses, and general support.

9 References

Abbott, B. W., Gruau, G., Zarnetske, J. P., Moatar, F., Barbe, L., Thomas, Z., Fovet, O., Kolbe, T., Gu, S., Pierson-Wickmann, A.-C., Davy, P., and Pinay, G.: Unexpected spatial stability of water chemistry in headwater stream networks, Ecol. Lett., 21, 296–308, https://doi.org/10.1111/ele.12897, 2018.

Aho, K., Kriloff, C., Godsey, S.E., Ramos, R., Wheeler, C., You, Y., Warix, S., Derryberry, D., Zipper, S., Hale, R.L., Bond, C.T., and Kuehn, K.A.: Non-perennial stream networks as directed acyclic graphs: The R-package streamDAG. Environ. Modell. Softw. 167, 105775 https://doi.org/10.1016/j.envsoft.2023.105775, 2023.





- Allen, D. C., Busch, M.: AIMS SOP Macroinvertebrate Field Sampling, HydroShare,
- 695 http://www.hydroshare.org/resource/aa520613634347c09b4379385589eb8f, 2025.
 - APHA: Standard methods for the examination of water and wastewater (23rd ed.). American Public Health Association. 2017.
- Bernal, S., Cohen, M. J., Ledesma, J. L. J., Kirk, L., Martí, E., and Lupon, A.: Stream metabolism sources a large fraction of carbon dioxide to the atmosphere in two hydrologically contrasting headwater streams, Limnol. Oceanogr., 67, 2621–2634, https://doi.org/10.1002/lno.12226, 2022.
 - Bernal, S., Ledesma, J. L. J., Peñarroya, X., Jativa, C., Catalán, N., Casamayor, E. O., Lupon, A., Marcé, R., Martí, E., Triadó-Margarit, X., and Rocher-Ros, G.: Expanding towards contraction: the alternation of floods and droughts as a fundamental component in river ecology, Biogeochemistry, 168, 11, https://doi.org/10.1007/s10533-024-01197-1, 2025.
- Bieroza, M., Acharya, S., Benisch, J., ter Borg, R. N., Hallberg, L., Negri, C., Pruitt, A., Pucher, M., Saavedra, F.,
 Staniszewska, K., van't Veen, S. G. M., Vincent, A., Winter, C., Basu, N. B., Jarvie, H. P., and Kirchner, J. W.: Advances in Catchment Science, Hydrochemistry, and Aquatic Ecology Enabled by High-Frequency Water Quality Measurements,
 Environ. Sci. Technol., 57, 4701–4719, https://doi.org/10.1021/acs.est.2c07798, 2023.
- Blaen, P. J., Khamis, K., Lloyd, C. E. M., Bradley, C., Hannah, D., and Krause, S.: Real-time monitoring of nutrients and dissolved organic matter in rivers: Capturing event dynamics, technological opportunities and future directions, Sci. Total
 Environ., 569–570, 647–660, https://doi.org/10.1016/j.scitotenv.2016.06.116, 2016.
 - Bokulich, N. A. and Mills, D. A.: Improved selection of internal transcribed spacer-specific primers enables quantitative, ultra-high-throughput profiling of fungal communities, Appl. Environ. Microbiol., 79, 2519–2526, https://doi.org/10.1128/AEM.03870-12, 2013.
- Bond, C. T., Nave, B. A., Kemajou Tchamba, A. L., Stanley, E., Zeglin, L. H., Jackson, C. R., Zipper, S., Aho, K., Burgin, A. J., You, Y., Ramos, R., and Kuehn K. A.: Fungal communities across a surface water permanence gradient in a non-perennial prairie stream network, ISME Communications, 5, ycaf151, https://doi.org/10.1093/ismeco/ycaf151, 2025.
 - Brinkerhoff, C. B., Gleason, C. J., Kotchen, M. J., Kysar, D. A., and Raymond, P. A.: Ephemeral stream water contributions to United States drainage networks, Science, 384, 1476–1482, https://doi.org/10.1126/science.adg9430, 2024.
 - Burgin, A. J.: AIMS_SOP_Surface Water Chemistry Field Sampling, HydroShare,
- 720 https://doi.org/10.4211/hs.ac0c4f31e8a64c52bae41e5719bd3c14, 2024.





- Burgin, A. J., Zarek, K., Wilhelm, J., and Flynn, S.: AIMS Dissolved Gas Field Sampling SOP, HydroShare, http://www.hydroshare.org/resource/9443322b95784f399cd133da1be948d9, 2025.
- Burke, E., Wilhelm, J., Zipper, S., and Brown, C. L.: AIMS SOP STIC Calibration, HydroShare, http://www.hydroshare.org/resource/9f2027c779d64149be32bdb9eede54f2, 2024.
- Busch, M. H., Costigan, K. H., Fritz, K. M., Datry, T., Krabbenhoft, C. A., Hammond, J. C., Zimmer, M., Olden, J. D., Burrows, R. M., Dodds, W. K., Boersma, K. S., Shanafield, M., Kampf, S. K., Mims, M. C., Bogan, M. T., Ward, A. S., Perez Rocha, M., Godsey, S., Allen, G. H., Blaszczak, J. R., Jones, C. N., and Allen, D. C.: What's in a Name? Patterns, Trends, and Suggestions for Defining Non-Perennial Rivers and Streams, Water, 12, https://doi.org/10.3390/w12071980, 2020.
- Clark, J. B., Neale, P., Tzortziou, M., Cao, F., and Hood, R. R.: A mechanistic model of photochemical transformation and degradation of colored dissolved organic matter, Mar. Chem., 214, 103666, https://doi.org/10.1016/j.marchem.2019.103666, 2019.
 - Coble, P. G.: Characterization of marine and terrestrial DOM in seawater using excitation-emission matrix spectroscopy, Mar. Chem., 51, 325–346, https://doi.org/10.1016/0304-4203(95)00062-3, 1996.
- Cook, T. A.: Stratigraphy and structure of the central Talladega slate belt, Alabama Appalachians, in: Tectonic Studies in the Talladega and Carolina Slate Belts, Southern Appalachian Orogen, vol. 191, edited by: Bearce, D. N., Black, W. W., Kish, S. A., and Tull, J. F., Geological Society of America, 0, https://doi.org/10.1130/SPE191-p47, 1982.
 - Datry, T., Truchy, A., Olden, J. D., Busch, M. H., Stubbington, R., Dodds, W. K., Zipper, S., Yu, S., Messager, M. L., Tonkin, J. D., Kaiser, K. E., Hammond, J. C., Moody, E. K., Burrows, R. M., Sarremejane, R., DelVecchia, A. G., Fork, M.
- L., Little, C. J., Walker, R. H., Walters, A. W., and Allen, D.: Causes, Responses, and Implications of Anthropogenic versus Natural Flow Intermittence in River Networks, BioScience, 73, 9–22, https://doi.org/10.1093/biosci/biac098, 2023.
 - Downing, B. D., Pellerin, B. A., Bergamaschi, B. A., Saraceno, J. F., and Kraus, T. E. C.: Seeing the light: The effects of particles, dissolved materials, and temperature on in situ measurements of DOM fluorescence in rivers and streams, Limnol. Oceanogr. Methods, 10, 767–775, https://doi.org/10.4319/lom.2012.10.767, 2012.
- 745 Exo User Manual. Advanced water quality monitoring platform, YSI, a xylem brand. 2020.





- Fellman, J. B., Hood, E., and Spencer, R. G. M.: Fluorescence spectroscopy opens new windows into dissolved organic matter dynamics in freshwater ecosystems: A review, Limnol. Oceanogr., 55, 2452–2462, https://doi.org/10.4319/lo.2010.55.6.2452, 2010.
- Feminella, J. W.: Comparison of Benthic Macroinvertebrate Assemblages in Small Streams along a Gradient of Flow Permanence, J. North Am. Benthol. Soc., 15, 651–669, https://doi.org/10.2307/1467814, 1996.
 - Gibson, J. F., Shokralla, S., Curry, C., Baird, D. J., Monk, W. A., King, I., and Hajibabaei, M.: Large-Scale Biomonitoring of Remote and Threatened Ecosystems via High-Throughput Sequencing, PLOS ONE, 10, e0138432, https://doi.org/10.1371/journal.pone.0138432, 2015.
- Godsey, S. E., Wheeler, C., and Zipper, S.: AIMS SOP STIC Deployment and Maintenance, HydroShare, http://www.hydroshare.org/resource/c82a87a6c63445029d35131260241386, 2024a.
 - Godsey, S. E., E. Seybold, E. C., Wolford, M. A., and Zipper, S.: AIMS SOP Streamflow Measurements Dilution gaging method, HydroShare, http://www.hydroshare.org/resource/5b1cbefc8ff94a26a652447838869f13, 2024b.
- Gómez, R., Arce, M. I., Baldwin, D. S., and Dahm, C. N.: Chapter 3.1 Water Physicochemistry in Intermittent Rivers and Ephemeral Streams, in: Intermittent Rivers and Ephemeral Streams, edited by: Datry, T., Bonada, N., and Boulton, A.,
 Academic Press, 109–134, https://doi.org/10.1016/B978-0-12-803835-2.00005-X, 2017.
 - Gómez-Gener, L., Siebers, A. R., Arce, M. I., Arnon, S., Bernal, S., Bolpagni, R., Datry, T., Gionchetta, G., Grossart, H.-P., Mendoza-Lera, C., Pohl, V., Risse-Buhl, U., Shumilova, O., Tzoraki, O., von Schiller, D., Weigand, A., Weigelhofer, G., Zak, D., and Zoppini, A.: Towards an improved understanding of biogeochemical processes across surface-groundwater interactions in intermittent rivers and ephemeral streams, Earth-Sci. Rev., 220, 103724,
- 765 https://doi.org/10.1016/j.earscirev.2021.103724, 2021.
 - Gore, J. A. and Banning, J.: Chapter 3 Discharge Measurements and Streamflow Analysis, in: Methods in Stream Ecology, Volume 1 (Third Edition), edited by: Hauer, F. R. and Lamberti, G. A., Academic Press, Boston, 49–70, https://doi.org/10.1016/B978-0-12-416558-8.00003-2, 2017.
- Griffith, G. E., Omernik, J. M., Comstock, J. A., Lawrence, S., Martin, G., Goddard, A., et al.: Ecoregions of Alabama. U.S.
 Environmental Protection Agency, National Health and Environmental Effects. Research Laboratory, Corvallis, OR.
 Retrieved from https://www.epa.gov/eco-research/ecoregion-download-files-state-region-4#pane-01, 2001.





- Hajibabaei, M., Spall, J. L., Shokralla, S., and van Konynenburg, S.: Assessing biodiversity of a freshwater benthic macroinvertebrate community through non-destructive environmental barcoding of DNA from preservative ethanol, BMC Ecol., 12, 28, https://doi.org/10.1186/1472-6785-12-28, 2012.
- Helms, J. R., Stubbins, A., Ritchie, J. D., Minor, E. C., Kieber, D. J., and Mopper, K.: Absorption spectral slopes and slope ratios as indicators of molecular weight, source, and photobleaching of chromophoric dissolved organic matter, Limnol. Oceanogr., 53, 955–969, https://doi.org/10.4319/lo.2008.53.3.0955, 2008.
 - Jackson, C. R., Tyler, H. L., and Millar, J. J.: Determination of Microbial Extracellular Enzyme Activity in Waters, Soils, and Sediments using High Throughput Microplate Assays, J. Vis. Exp., e50399, https://doi.org/10.3791/50399, 2013.
- Jackson, E. F., Echlin, H. L., and Jackson, C. R.: Changes in the phyllosphere community of the resurrection fern, Polypodium polypodioides, associated with rainfall and wetting, FEMS Microbiol. Ecol., 58, 236–246, https://doi.org/10.1111/j.1574-6941.2006.00152.x, 2006.
 - Kelly, M.: mimsy: Calculate MIMS Dissolved Gas Concentrations Without Getting a Headache. R package version 0.6.2. https://CRAN.R-project.org/package=mimsy, 2020.
- Kopaska-Merkel, D. C., Dean, L. S., and Moore, J. D.: Hydrogeology and vulnerability to contamination of major aquifers in Alabama: Area 5. Retrieved from https://www.ogb.alabama.gov/Home/DownloadPubDocument/?path=Circulars&fileName=C199C.pdf, 2000.
 - Kozich, J. J., Westcott, S. L., Baxter, N. T., Highlander, S. K., and Schloss, P. D.: Development of a dual-index sequencing strategy and curation pipeline for analyzing amplicon sequence data on the MiSeq Illumina sequencing platform, Appl.
- 790 Environ. Microbiol., 79, 5112–5120, https://doi.org/10.1128/AEM.01043-13, 2013.
 - Krabbenhoft, C. A., Allen, G. H., Lin, P., Godsey, S. E., Allen, D. C., Burrows, R. M., DelVecchia, A. G., Fritz, K. M., Shanafield, M., Burgin, A. J., Zimmer, M. A., Datry, T., Dodds, W. K., Jones, C. N., Mims, M. C., Franklin, C., Hammond, J. C., Zipper, S., Ward, A. S., Costigan, K. H., Beck, H. E., and Olden, J. D.: Assessing placement bias of the global river gauge network, Nat. Sustain., 5, 586–592, https://doi.org/10.1038/s41893-022-00873-0, 2022.
- Lane, C. R., Creed, I. F., Golden, H. E., Leibowitz, S. G., Mushet, D. M., Rains, M. C., Wu, Q., D'Amico, E., Alexander, L. C., Ali, G. A., Masu, N. B., Bennett, M. G., Christensen, J. R., Cohen, M. J., Covino, T. P., DeVries, B., Hill, R. A., Jencso, K., Lang, M. W., McLaughlin, D. L., Rosenberry, D. O., Rover, J., and Vanderhoof, M. K.: Vulnerable waters are essential to watershed resilience, Ecosystems, 26, 1-28, https://doi.org/10.1007/s10021-021-00737-2, 2023.





- Li, P. and Hur, J.: Utilization of UV-Vis spectroscopy and related data analyses for dissolved organic matter (DOM) studies:

 800 A review, Crit. Rev. Environ. Sci. Technol., 47, 131–154, https://doi.org/10.1080/10643389.2017.1309186, 2017.
 - López-Rojo, N., Sarremejane, R., Foulquier, A., Singer, G., Diamond, J., Rioux, D., Miquel, C., Mulero, S., Lionnet, C., Peñas, F. J., Rodeles, A. A., and Datry, T.: Alternating Drying and Flowing Phases Control Stream Metabolism Through Short- and Long-Term Effects: Insights From a River Network, J. Geophys. Res. Biogeosciences, 130, e2024JG008369, https://doi.org/10.1029/2024JG008369, 2025.
- Marcé, R., Obrador, B., Gómez-Gener, L., Catalán, N., Koschorreck, M., Arce, M. I., Singer, G., and von Schiller, D.: Emissions from dry inland waters are a blind spot in the global carbon cycle, Earth-Sci. Rev., 188, 240–248, https://doi.org/10.1016/j.earscirev.2018.11.012, 2019.
 - McCleskey, R. B., Runkel, R. L., Murphy, S. F., and Roth, D. A.: Stream Discharge Determinations Using Slug Additions and Specific Conductance, Water Resour. Res., 61, e2024WR037771, https://doi.org/10.1029/2024WR037771, 2025.
- McKnight, D. M., Boyer, E. W., Westerhoff, P. K., Doran, P. T., Kulbe, T., and Andersen, D. T.: Spectrofluorometric characterization of dissolved organic matter for indication of precursor organic material and aromaticity, Limnol. Oceanogr., 46, 38–48, https://doi.org/10.4319/lo.2001.46.1.0038, 2001.
- Messager, M. L., Lehner, B., Cockburn, C., Lamouroux, N., Pella, H., Snelder, T., Tockner, K., Trautmann, T., Watt, C., and Datry, T.: Global prevalence of non-perennial rivers and streams, Nature, 594, 391–397, https://doi.org/10.1038/s41586-021-03565-5, 2021.
 - Meyer, J. L., Strayer, D. L., Wallace, J. B., Eggert, S. L., Helfman, G. S., and Leonard, N. E.: The Contribution of Headwater Streams to Biodiversity in River Networks1, JAWRA J. Am. Water Resour. Assoc., 43, 86–103, https://doi.org/10.1111/j.1752-1688.2007.00008.x, 2007.
- Meyns, S., Illi, R., and Ribi, B.: Comparison of chlorophyll-a analysis by HPLC and spectrophotometry: Where do the differences come from?, Arch. Für Hydrobiol., 132, 129–139, https://doi.org/10.1127/archiv-hydrobiol/132/1994/129, 1994.
 - Murphy, J. and Riley, J. P.: A modified single solution method for the determination of phosphate in natural waters, Anal. Chim. Acta, 27, 31–36, https://doi.org/10.1016/S0003-2670(00)88444-5, 1962.
 - Ohno, T.: Fluorescence Inner-Filtering Correction for Determining the Humification Index of Dissolved Organic Matter, Environ. Sci. Technol., 36, 742–746, https://doi.org/10.1021/es0155276, 2002.





- Peterson, D. M., and Jones, C. N.: Talladega Environmental Data (AIMS_SE_TAL_ENVI), HydroShare, http://www.hydroshare.org/resource/81c003a7b8474d63a31641a4f375fd18, 2025a.
 - Peterson, D. M., and Jones, C. N.: Paint Rock Environmental Data (AIMS_SE_PRF_ENVI), HydroShare, http://www.hydroshare.org/resource/656211b1a1484433a3bc524fb968b4bd, 2025b.
- Peterson, D. M., and Jones, C. N.: Shambley Creek Environmental Data (AIMS_SE_WHR_ENVI), HydroShare, http://www.hydroshare.org/resource/126d2c7b1c8d4889a8ccc454d387b0d8, 2025c.
 - Poff, N. L.: Landscape Filters and Species Traits: Towards Mechanistic Understanding and Prediction in Stream Ecology, J. North Am. Benthol. Soc., 16, 391–409, https://doi.org/10.2307/1468026, 1997.
 - Ponta, G.: Geologic Framework of Karst Aquifer Systems in Alabama. Sinkhole Conference 2018. Retrieved from digitalcommons.usf.edu/sinkhole 2018/ProceedingswithProgram/Appalachian Karst/6, 2018.
- Pucher, M., Wünsch, U., Weigelhofer, G., Murphy, K., Hein, T., and Graeber, D.: staRdom: Versatile Software for Analyzing Spectroscopic Data of Dissolved Organic Matter in R, Water, 11, https://doi.org/10.3390/w11112366, 2019.
 - Rognes, T., Flouri, T., Nichols, B., Quince, C., and Mahé, F.: VSEARCH: a versatile open source tool for metagenomics. PeerJ, 4, e2584. https://doi.org/10.7717/peerj.2584, 2016.
- Rolls, R. J., Heino, J., Ryder, D. S., Chessman, B. C., Growns, I. O., Thompson, R. M., and Gido, K. B.: Scaling biodiversity responses to hydrological regimes, Biol. Rev., 93, 971–995, https://doi.org/10.1111/brv.12381, 2018.
 - Ruhala, S. S. and Zarnetske, J. P.: Using in-situ optical sensors to study dissolved organic carbon dynamics of streams and watersheds: A review, Sci. Total Environ., 575, 713–723, https://doi.org/10.1016/j.scitotenv.2016.09.113, 2017.
 - Ruhí, A., Datry, T., and Sabo, J. L.: Interpreting beta-diversity components over time to conserve metacommunities in highly dynamic ecosystems, Conserv. Biol., 31, 1459–1468, https://doi.org/10.1111/cobi.12906, 2017.
- Senatore, A., Corrente, G. A., Argento, E. L., Castagna, J., Micieli, M., Mendicino, G., Beneduci, A., and Botter, G.: Seasonal and Storm Event-Based Dynamics of Dissolved Organic Carbon (DOC) Concentration in a Mediterranean Headwater Catchment, Water Resour. Res., 59, e2022WR034397, https://doi.org/10.1029/2022WR034397, 2023.
 - Seybold, E. C.: AIMS_SOP_waterQualSensorInstall, HydroShare, https://doi.org/10.4211/hs.703cf05242f7455c8dfb072dd072c962, 2024.





- Shogren, A. J., Zarnetske, J. P., Abbott, B. W., Bratsman, S., Brown, B., Carey, M. P., Fulweber, R., Greaves, H. E., Haines, E., Iannucci, F., Koch, J. C., Medvedeff, A., O'Donnell, J. A., Patch, L., Poulin, B. A., Williamson, T. J., and Bowden, W. B.: Multi-year, spatially extensive, watershed-scale synoptic stream chemistry and water quality conditions for six permafrost-underlain Arctic watersheds, Earth Syst. Sci. Data, 14, 95–116, https://doi.org/10.5194/essd-14-95-2022, 2022.
- Soil Survey Staff, Natural Resources Conservation Service, United States Department of Agriculture. (n.d.). Web Soil Survey [Data set]. Retrieved from https://websoilsurvey.nrcs.usda.gov/app/
 - Solórzano, L.: Determination of ammonia in natural waters by the phenolhypochlorite method, Limnol. Oceanogr., 14, 799–801, https://doi.org/10.4319/lo.1969.14.5.0799, 1969.
 - Swenson, L. J., Zipper, S., Peterson, D. M., Jones, C. N., Burgin, A. J., Seybold, E., Kirk, M. F., and Hatley, C.: Changes in Water Age During Dry-Down of a Non-Perennial Stream, Water Resour. Res., 60, e2023WR034623,
- 860 https://doi.org/10.1029/2023WR034623, 2024.
 - Szabo, E. W., Osborne, W. E., Copeland, C. W., and Neathery, T. L.: Geologic map of Alabama. Geological Survey of Alabama. Retrieved from https://ngmdb.usgs.gov/Prodesc/proddesc_55859.htm, 1988.
- Thompson, L. R., Sanders, J. G., McDonald, D., Amir, A., Ladau, J., Locey, K. J., Prill, R. J., Tripathi, A., Gibbons, S. M., Ackermann, G., Navas-Molina, J. A., Janssen, S., Kopylova, E., Vázquez-Baeza, Y., González, A., Morton, J. T., Mirarab, S., Zech Xu, Z., Jiang, L., Haroon, M. F., Kanbar, J., Zhu, Q., Jin Song, S., Kosciolek, T., Bokulich, N. A., Lefler, J.,
- Brislawn, C. J., Humphrey, G., Owens, S. M., Hampton-Marcell, J., Berg-Lyons, D., McKenzie, V., Fierer, N., Fuhrman, J. A., Clauset, A., Stevens, R. L., Shade, A., Pollard, K. S., Goodwin, K. D., Jansson, J. K., Gilbert, J. A., Knight, R., Rivera, J.
 - L. A., Al-Moosawi, L., Alverdy, J., Amato, K. R., Andras, J., Angenent, L. T., Antonopoulos, D. A., Apprill, A., Armitage, D., Ballantine, K., Bárta, J., Baum, J. K., Berry, A., Bhatnagar, A., Bhatnagar, M., Biddle, J. F., Bittner, L., Boldgiv, B.,
- Bottos, E., Boyer, D. M., Braun, J., Brazelton, W., Brearley, F. Q., Campbell, A. H., Caporaso, J. G., Cardona, C., Carroll, J., Cary, S. C., Casper, B. B., Charles, T. C., Chu, H., Claar, D. C., Clark, R. G., Clayton, J. B., Clemente, J. C., Cochran, A., Coleman, M. L., Collins, G., Colwell, R. R., Contreras, M., Crary, B. B., Creer, S., Cristol, D. A., Crump, B. C., Cui, D.,
- Daly, S. E., Davalos, L., Dawson, R. D., Defazio, J., Delsuc, F., Dionisi, H. M., Dominguez-Bello, M. G., Dowell, R.,
 Dubinsky, E. A., Dunn, P. O., Ercolini, D., Espinoza, R. E., et al.: A communal catalogue reveals Earth's multiscale
 microbial diversity, Nature, 551, 457–463, https://doi.org/10.1038/nature24621, 2017.
 - Tramblay, Y., Rutkowska, A., Sauquet, E., Sefton, C., Laaha, G., Osuch, M., Albuquerque, T., Alves, M. H., Banasik, K., Beaufort, A., Brocca, L., Camici, S., Csabai, Z., Dakhlaoui, H., DeGirolamo, A. M., Dörflinger, G., Gallart, F., Gauster, T.,



885

2019, 2019a.



- Hanich, L., Kohnová, S., Mediero, L., Plamen, N., Parry, S., Quintana-Seguí, P., Tzoraki, O., and Datry, T.: Trends in flow intermittence for European rivers, Hydrol. Sci. J., 66, 37–49, https://doi.org/10.1080/02626667.2020.1849708, 2021.
- Walsh, R. and Ward, A. S.: An overview of the evolving jurisdictional scope of the U.S. Clean Water Act for hydrologists, WIREs Water, 9, e1603, https://doi.org/10.1002/wat2.1603, 2022.
 - Ward, A. S., Zarnetske, J. P., Baranov, V., Blaen, P. J., Brekenfeld, N., Chu, R., Derelle, R., Drummond, J., Fleckenstein, J. H., Garayburu-Caruso, V., Graham, E., Hannah, D., Harman, C. J., Herzog, S., Hixson, J., Knapp, J. L. A., Krause, S., Kurz, M. J., Lewandowski, J., Li, A., Martí, E., Miller, M., Milner, A. M., Neil, K., Orsini, L., Packman, A. I., Plont, S., Renteria, L., Roche, K., Royer, T., Schmadel, N. M., Segura, C., Stegen, J., Toyoda, J., Hager, J., Wisnoski, N. I., and Wondzell, S. M.: Co-located contemporaneous mapping of morphological, hydrological, chemical, and biological conditions in a 5th-order mountain stream network, Oregon, USA, Earth Syst. Sci. Data, 11, 1567–1581, https://doi.org/10.5194/essd-11-1567-
- Ward, A. S., Wondzell, S. M., Schmadel, N. M., Herzog, S., Zarnetske, J. P., Baranov, V., Blaen, P. J., Brekenfeld, N., Chu, R., Derelle, R., Drummond, J., Fleckenstein, J. H., Garayburu-Caruso, V., Graham, E., Hannah, D., Harman, C. J., Hixson, J., Knapp, J. L. A., Krause, S., Kurz, M. J., Lewandowski, J., Li, A., Martí, E., Miller, M., Milner, A. M., Neil, K., Orsini, L., Packman, A. I., Plont, S., Renteria, L., Roche, K., Royer, T., Segura, C., Stegen, J., Toyoda, J., Hager, J., and Wisnoski, N. I.: Spatial and temporal variation in river corridor exchange across a 5th-order mountain stream network, Hydrol. Earth Syst. Sci., 23, 5199–5225, https://doi.org/10.5194/hess-23-5199-2019, 2019b.
- Watras, C. J., Hanson, P. C., Stacy, T. L., Morrison, K. M., Mather, J., Hu, Y.-H., and Milewski, P.: A temperature compensation method for CDOM fluorescence sensors in freshwater, Limnol. Oceanogr. Methods, 9, 296–301, https://doi.org/10.4319/lom.2011.9.296, 2011.
 - Weishaar, J. L., Aiken, G. R., Bergamaschi, B. A., Fram, M. S., Fujii, R., and Mopper, K.: Evaluation of Specific Ultraviolet Absorbance as an Indicator of the Chemical Composition and Reactivity of Dissolved Organic Carbon, Environ. Sci. Technol., 37, 4702–4708, https://doi.org/10.1021/es030360x, 2003.
 - Weiss, R. F.: Carbon dioxide in water and seawater: the solubility of a non-ideal gas, Mar. Chem., 2, 203–215, https://doi.org/10.1016/0304-4203(74)90015-2, 1974.
 - Weiss, R. F. and Price, B. A.: Nitrous oxide solubility in water and seawater, Mar. Chem., 8, 347–359, https://doi.org/10.1016/0304-4203(80)90024-9, 1980.





Wiesenburg, D. A. and Guinasso, N. L. Jr.: Equilibrium solubilities of methane, carbon monoxide, and hydrogen in water and sea water, J. Chem. Eng. Data, 24, 356–360, https://doi.org/10.1021/je60083a006, 1979.

Wu, Q., and Brown, A.: *whitebox: WhiteboxTools R Frontend*. R package version 2.2.0, https://CRAN.R-project.org/package=whitebox, 2022.

You, Y., Kerner, P., Shanmugam, S., and Khodakovskaya, M. V.: Emerging investigator series: differential effects of carbon nanotubes and graphene on the tomato rhizosphere microbiome, Environmental Science: Nano, 10, 1570–1584, https://doi.org/10.1039/D2EN01026G

Zarek, K., Jones, C. N., Peterson, D. M., Plont, S., Shogren, A. J., Tatariw, C., Speir, S. L., Mortazavi, B., and Burgin, A. J.: Investigating Spatial and Temporal Nitrogen Dynamics in a Forested Headwater Stream Over the Course of an Annual Drying Event, J. Geophys. Res. Biogeosciences, 130, e2024JG008522, https://doi.org/10.1029/2024JG008522, 2025a.

915 Zarek, K., and Burgin, A. J.: AIMS SOP MIMS Field Sampling, HydroShare, http://www.hydroshare.org/resource/3ddde3893761475fa9dd1f758a501ccc, 2025.

Zeglin, L., and Busch, M. H.: AIMS SOP - Microbial Field Sampling, HydroShare, http://www.hydroshare.org/resource/4b071711215341118330c22f18b5d20d, 2024.

Zimmer, M. A., Burgin, A. J., Kaiser, K., and Hosen, J.: The unknown biogeochemical impacts of drying rivers and streams, Nat. Commun., 13, 7213, https://doi.org/10.1038/s41467-022-34903-4, 2022.

Zipper, S., Wheeler, C. T., and Godsey, S. E.: AIMS SOP Pressure Transducers, HydroShare, http://www.hydroshare.org/resource/2ed03f228a2a415889c33c59b1427972, 2025a.

Zipper, S., Wheeler, C. T., Peterson, D. M., Cook, S. C., Godsey, S. E., and Aho, K.: STICr: An open-source package and workflow for stream temperature, intermittency, and conductivity (STIC) data, Environ. Model. Softw., 190, 106484, https://doi.org/10.1016/j.envsoft.2025.106484, 2025b.

Zipper, S. C., Hammond, J. C., Shanafield, M., Zimmer, M., Datry, T., Jones, C. N., Kaiser, K. E., Godsey, S. E., Burrows, R. M., Blaszczak, J. R., Busch, M. H., Price, A. N., Boersma, K. S., Ward, A. S., Costigan, K., Allen, G. H., Krabbenhoft, C. A., Dodds, W. K., Mims, M. C., Olden, J. D., Kampf, S. K., Burgin, A. J., and Allen, D. C.: Pervasive changes in stream intermittency across the United States, Environ. Res. Lett., 16, 084033, https://doi.org/10.1088/1748-9326/ac14ec, 2023.

930

925





Appendix A

Table A1: Citations associated with each Data Product Citation Identifier listed in Table 2, Table 3, and Table 4.

Data Product Citation Identifier	Data Product Citation
TAL_ENVI	Peterson, D., N. Jones (2025). Talladega Environmental Data (AIMS_SE_TAL_ENVI), HydroShare, http://www.hydroshare.org/resource/81c003a7b8474d63a31641a4f375fd18
PRF_ENVI	Peterson, D., N. Jones (2025). Paint Rock Environmental Data (AIMS_SE_PRF_ENVI), HydroShare, http://www.hydroshare.org/resource/656211b1a1484433a3bc524fb968b4bd
WHR_ENVI	Peterson, D., N. Jones (2025). Shambley Creek Environmental Data (AIMS_SE_WHR_ENVI), HydroShare, http://www.hydroshare.org/resource/126d2c7b1c8d4889a8ccc454d387b0d8
TAL_METS	Peterson, D., N. Jones (2025). Talladega Meteorological Data (AIMS_SE_TAL_approach1_METS), HydroShare, http://www.hydroshare.org/resource/281cd7627629481dbdc7d4ccf6fcfbcc
PRF_METS	Peterson, D., N. Jones (2025). Paint Rock Meteorological Data (AIMS_SE_PRF_approach1_METS), HydroShare, http://www.hydroshare.org/resource/4089918c0a494bfeb19be0421a33d297
WHR_METS	Peterson, D., N. Jones (2025). Shambley Creek Meteorological Data (AIMS_SE_WHR_approach1_METS), HydroShare, http://www.hydroshare.org/resource/33823d8603ce439fbba48fbcbba22da4
TAL_STIC	Peterson, D., N. Jones (2025). Talladega Stream Temperature, Intermittency, and Conductivity Data (AIMS_SE_TAL_approach1_STIC), HydroShare, http://www.hydroshare.org/resource/ff306bec9fb24e52aa809dbb4d074731
PRF_STIC	Peterson, D., N. Jones (2025). Paint Rock Stream Temperature, Intermittency, and Conductivity Data (AIMS_SE_PRF_approach1_STIC), HydroShare, http://www.hydroshare.org/resource/d57338ebfb0240f58e8de37ddacf9426
WHR_STIC	Peterson, D., N. Jones (2025). Shambley Creek Stream Temperature, Intermittency, and Conductivity Data (AIMS_SE_WHR_approach1_STIC), HydroShare, http://www.hydroshare.org/resource/dc623510ed1847f8abe1275904472c44
TAL_PRES	Peterson, D., N. Jones (2025). Talladega Pressure Transducer Data (AIMS_SE_TAL_approach1_PRES), HydroShare, http://www.hydroshare.org/resource/93e2861410e647d9a710eea036832dbe
PRF_PRES	Peterson, D., N. Jones (2025). Paint Rock Pressure Transducer Data (AIMS_SE_PRF_approach1_PRES), HydroShare, http://www.hydroshare.org/resource/a45b5e24dafc4a76a665405664afada7
WHR_PRES	Peterson, D., N. Jones (2025). Shambley Creek Pressure Transducer Data (AIMS_SE_WHR_approach1_PRES), HydroShare, http://www.hydroshare.org/resource/bc34c8b51c514bf4a6e0a44493bf8ca3
TAL_DISC	Plont, S., M. Wolford, K. Zarek, D. Peterson, N. Jones, S. Speir (2025). AIMS Talladega Continuous Discharge at Watershed Outlet Data (AIMS_SE_TAL_DISC), HydroShare, http://www.hydroshare.org/resource/fc7ae2d28e3c481d805902a79af90a95





PRF_DISC	Plont, S., S. Speir, D. Peterson, N. Jones (2025). AIMS Paint Rock Continuous Discharge at Watershed Outlet Data (AIMS_SE_PRF_DISC), HydroShare, http://www.hydroshare.org/resource/043fc07f0c3b47bcabbd0bf5600d929f
WHR_DISC	Plont, S., S. Speir, D. Peterson, N. Jones (2025). AIMS Shambley Creek Continuous Discharge at Watershed Outlet Data (AIMS_SE_WHR_DISC), HydroShare, http://www.hydroshare.org/resource/535797126b134ceaab9838df0ca00885
TAL_EXOS	Plont, S., M. Wolford, K. Zarek, S. Speir, C. Smith (2025). AIMS Talladega Continuous Water Quality at Watershed Outlet Data (AIMS_SE_TAL_EXOS), HydroShare, http://www.hydroshare.org/resource/9e47c3dfc549446e80173dfe6ac48365
PRF_EXOS	Plont, S., M. Wolford, K. Zarek, S. Speir, C. Smith (2025). AIMS Paint Rock Continuous Water Quality at Watershed Outlet Data (AIMS_SE_PRF_EXOS), HydroShare, http://www.hydroshare.org/resource/aeb715ff9c7b4f1098bdebc0fd9e9551
WHR_EXOS	Plont, S., M. Wolford, D. Peterson, S. Speir, C. Smith, K. Zarek (2025). AIMS Shambley Creek Continuous Water Quality at Watershed Outlet Data (AIMS_SE_WHR_EXOS), HydroShare, http://www.hydroshare.org/resource/a7bdb79e06684db2886a257ec614018a
TAL_SCAN	Plont, S., M. Wolford, K. Zarek, S. Speir (2025). AIMS Talladega Absorbance Spectral Fingerprint at Watershed Outlet (AIMS_SE_TAL_SCAN), HydroShare, http://www.hydroshare.org/resource/cea7ec0e055f49ef9f55fc61caffc52a
TAL_YSIS	Plont, S., M. Wolford, S. Speir, D. Peterson, K. Zarek, C. Smith, C. Atkinson (2025). AIMS Talladega Field Physicochemistry Data and Field Notes (AIMS_SE_TAL_YSIS), HydroShare, http://www.hydroshare.org/resource/e36dc69dca0e4fbc969e7ae6137f3744
PRF_YSIS	Plont, S., M. Wolford, S. Speir, D. Peterson, K. Zarek, C. Smith, C. Atkinson (2025). AIMS Paint Rock Field Physicochemistry Data and Field Notes (AIMS_SE_PRF_YSIS), HydroShare, http://www.hydroshare.org/resource/7fb2e1872cb840bcbcd8bd4e1ea12185
WHR_YSIS	Plont, S., M. Wolford, S. Speir, D. Peterson, K. Zarek, C. Smith, C. Atkinson (2025). AIMS Shambley Creek Field Physicochemistry Data and Field Notes (AIMS_SE_WHR_YSIS), HydroShare, http://www.hydroshare.org/resource/a9394fd2e0d748fbb3ca5c36b451c15f
TAL_DISL	Plont, S., D. Peterson, M. Wolford, N. Jones (2025). AIMS Talladega Field Discharge Data (AIMS_SE_TAL_DISL), HydroShare, http://www.hydroshare.org/resource/0e7ad0451bdc45d2b0a51bb538a10909
PRF_DISL	Plont, S., D. Peterson, N. Jones, S. Speir (2025). AIMS Paint Rock Field Discharge Data (AIMS_SE_PRF_DISL), HydroShare, http://www.hydroshare.org/resource/d52b989e537349019842dba236627b66
WHR_DISL	Plont, S., D. Peterson, N. Jones, S. Speir (2025). AIMS Shambley Creek Field Discharge Data (AIMS_SE_WHR_DISL), HydroShare, http://www.hydroshare.org/resource/eedcfcb232ee45a6915bd26c68e301e8
TAL_WAIS	Peterson, D., S. Plont, N. Jones (2025). Talladega Water Isotopes Data (AIMS_SE_TAL_WAIS), HydroShare, http://www.hydroshare.org/resource/5fffa420810f4945a7ee8d3f8bda3ad2
PRF_WAIS	Peterson, D., S. Plont, N. Jones (2025). Paint Rock Water Isotopes Data (AIMS_SE_PRF_WAIS), HydroShare, http://www.hydroshare.org/resource/2088b266609c4ac58195a9390598633e
WHR_WAIS	Peterson, D., S. Plont, N. Jones (2025). Shambley Creek Water Isotopes Data (AIMS_SE_WHR_WAIS), HydroShare, http://www.hydroshare.org/resource/3ac22e1bc2c547e8a8af4ebd753323e4
TAL_TSSS	Plont, S., S. Speir, C. Smith, C. L. Atkinson, M. Wolford (2025). AIMS Talladega Suspended Solids Data (AIMS_SE_TAL_TSSS), HydroShare, http://www.hydroshare.org/resource/b230a7995b06498cacd28106a3be0f35





PRF_TSSS	Plont, S., S. Speir, C. Smith, C. L. Atkinson (2025). AIMS Paint Rock Suspended Solids Data (AIMS_SE_PRF_TSSS), HydroShare, http://www.hydroshare.org/resource/3eaacf0102594482ae2451c60745d7e6
WHR_TSSS	Plont, S., S. Speir, C. Smith, C. L. Atkinson (2025). AIMS Shambley Creek Suspended Solids Data (AIMS_SE_WHR_TSSS), HydroShare, http://www.hydroshare.org/resource/1284a362f1f9410b87d91598afc53c83
TAL_NUTR	Smith, C., C. L. Atkinson, S. Speir, M. Wolford, T. Layman, S. Plont (2025). AIMS Talladega nutrient data (AIMS_SE_TAL_NUTR), HydroShare, http://www.hydroshare.org/resource/730b486c0ef14d78b678963ffecc1a39
PRF_NUTR	Smith, C., C. L. Atkinson, S. Plont, M. Wolford, S. Speir, T. Layman, C. Dorantes (2025). AIMS Paint Rock nutrient data (AIMS_SE_PRF_NUTR), HydroShare, http://www.hydroshare.org/resource/165f2b4d1903485d82304bbc55ecd715
WHR_NUTR	Smith, C., C. L. Atkinson, S. Plont, M. Wolford, S. Speir, T. Layman (2025). AIMS Shambley Creek nutrient data (AIMS_SE_WHR_NUTR), HydroShare, http://www.hydroshare.org/resource/c0008581efb741dda4156fa887c16eb5
TAL_DOCS	Plont, S., S. Speir, M. Wolford, N. Jones (2025). AIMS Talladega Dissolved Organic Carbon Data (AIMS_SE_TAL_DOCS), HydroShare, http://www.hydroshare.org/resource/e80e4db42de940aa9fe18667dddebec4
PRF_DOCS	Plont, S., S. Speir, M. Wolford, N. Jones (2025). AIMS Paint Rock Dissolved Organic Carbon Data (AIMS_SE_PRF_DOCS), HydroShare, http://www.hydroshare.org/resource/1efa655d91fe43c58f8acbf0f52545c8
WHR_DOCS	Plont, S., S. Speir, M. Wolford, N. Jones (2025). AIMS Shambley Creek Dissolved Organic Carbon Data (AIMS_SE_WHR_DOCS), HydroShare, http://www.hydroshare.org/resource/8b750838affc438e88bcb2cd0dfd5dbf
TAL_DOMS	Hale, R., E. Bilbrey, c. dorantes, M. Wolford, S. Plont, L. M. Serpas (2025). AIMS Talladega dissolved organic matter data (AIMS_SE_TAL_DOMS), HydroShare, http://www.hydroshare.org/resource/aa792fa579f5443bba4376008da9f48e
PRF_DOMS	Hale, R., E. Bilbrey, c. dorantes, M. Wolford, S. Plont, L. M. Serpa (2025). AIMS Paint Rock dissolved organic matter data (AIMS_SE_PRF_DOMS), HydroShare, http://www.hydroshare.org/resource/da3766f455944ef0a8613c20d2870d38
WHR_DOMS	Hale, R., E. Bilbrey, c. dorantes, M. Wolford, S. Plont, L. M. Serpas (2025). AIMS Shambley Creek dissolved organic matter data (AIMS_SE_WHR_DOMS), HydroShare, http://www.hydroshare.org/resource/b6142a7bfabe4be988733e2c59bd8533
TAL_ANIO	Seybold, E., A. J. Shogren, C. Smith, S. Plont, K. Zarek, C. L. Atkinson, M. Busch (2025). AIMS Talladega anion data (AIMS_SE_TAL_ANIO), HydroShare, http://www.hydroshare.org/resource/0decb1efb3a34e88b39b64dbb6369743
PRF_ANIO	Shogren, A. J., E. Seybold, C. Smith, S. Plont, K. Zarek, C. L. Atkinson, M. Busch (2025). AIMS Paint Rock anion data (AIMS_SE_PRF_ANIO), HydroShare, http://www.hydroshare.org/resource/e025fb27b18141beab4cebda71528efc
WHR_ANIO	Shogren, A. J., E. Seybold, C. Smith, S. Plont, K. Zarek, C. L. Atkinson, M. Busch (2025). AIMS Shambley Creek anion data (AIMS_SE_WHR_ANIO), HydroShare, http://www.hydroshare.org/resource/3a783ac086a74e6987dfefb870fb8cb3
TAL_CAIO	Seybold, E., S. Plont, M. Busch, c. dorantes (2025). AIMS Talladega Cation Data (AIMS_SE_TAL_CAIO), HydroShare, http://www.hydroshare.org/resource/dc0434b19c834941aa56449af0f6ce9b





PRF_CAIO	Seybold, E., S. Plont, M. Busch, c. dorantes (2025). AIMS Paint Rock Cation Data (AIMS_SE_PRF_CAIO), HydroShare, http://www.hydroshare.org/resource/0495c3eabb474b1190211fd278b4b467
WHR_CAIO	Seybold, E., S. Plont, M. Busch, c. dorantes (2025). AIMS Shambley Creek Cation Data (AIMS_SE_WHR_CAIO), HydroShare, http://www.hydroshare.org/resource/eb3f2e78492f4ec9bd5a11791712a6f9
TAL_MIMS	Zarek, K., A. Burgin, S. L. Speir, T. Layman (2025). AIMS Talladega Gases Data (AIMS_SE_TAL_MIMS), HydroShare, http://www.hydroshare.org/resource/5ff9056710d04917bd6891b46496d7b0
PRF_MIMS	Zarek, K., A. Burgin, T. Layman (2025). AIMS Paint Rock Gases Data (AIMS_SE_PRF_MIMS), HydroShare, http://www.hydroshare.org/resource/036b5916526347bc8bad0ad61559fb9e
WHR_MIMS	Zarek, K., A. Burgin, T. Layman (2025). AIMS Shambley Creek Gases data (AIMS_SE_WHR_MIMS), HydroShare, http://www.hydroshare.org/resource/c8b4f7ebda48424fad3d709a1b9372aa
TAL_GHGS	Burgin, A., c. dorantes, S. Plont (2025). AIMS Talladega Greenhouse Gas Data (AIMS_SE_TAL_GHGS), HydroShare, http://www.hydroshare.org/resource/34b55fc99e94410f8db6766511b448bb
SE_MIME	Bond, C. T., K. A. Kuehn (2025). AIMS_SE_approach2_approach3_MIME, HydroShare, http://www.hydroshare.org/resource/3161225427d8472d9f347068e1afab61
TAL_MAME	Smith, C., C. Atkinson, D. Allen (2025). AIMS Talladega macorinvertebrate field data(AIMS_SE_TAL_MAME), HydroShare, http://www.hydroshare.org/resource/549b107d949e43cba49adadfdc9b0c15
PRF_MAME	Smith, C., C. Atkinson, D. Allen (2025). AIMS Paint Rock macorinvertebrate field data (AIMS_SE_PRF_MAME), HydroShare, http://www.hydroshare.org/resource/21421686430f42ca9e9936fac26fffd3
WHR_MAME	Smith, C., C. Atkinson, D. Allen (2025). AIMS Shambley Creek macroinvertebrate field data (AIMS_SE_WHR_MAME), HydroShare, http://www.hydroshare.org/resource/b2f68f520074419f8e556585daa5b371
SE_AFDM	Bond, C. T., A. L. Kemajou Tchamba, K. A. Kuehn, C. R. Jackson (2025). AIMS_SE_approach2_approach3_AFDM, HydroShare, http://www.hydroshare.org/resource/df5dff9fd883414a8bf91ddeb268e514
SE_CHLA	Bond, C. T., A. Stafford, K. A. Kuehn (2025). Chlorophyll-a data from southeastern forest (AL, USA) seasonal and synoptic stream sampling (AIMS_SE_approach2_approach3_CHLA), HydroShare, http://www.hydroshare.org/resource/cd2852e4a0ca4e8d8d65dd3bcd7bd8ad
SE_MACR	Smith, C., D. Allen, C. Atkinson (2025). AIMS Southeast, macroinvertebrate sequences (AIMS_SE_MACR), HydroShare, http://www.hydroshare.org/resource/8f8d336d073343e7af1197d1ce6b6085
TAL_EEAS_A2	Kemajou Tchamba, A. L., C. R. Jackson (2025). AIMS_SE_Approach2_TAL_EEAS, HydroShare, http://www.hydroshare.org/resource/433c5de6768d4ad89f0027ad2101dcda
TAL_EEAS_A3	Kemajou Tchamba, A. L., C. R. Jackson (2025). AIMS_SE_approach3_EEAS, HydroShare, http://www.hydroshare.org/resource/eb7624d386584c1fb5468ed376487552
PRF_EEAS	Kemajou Tchamba, A. L., C. R. Jackson (2025). AIMS_SE_Approach2_PRF_EEAS, HydroShare, http://www.hydroshare.org/resource/3b2886a7bade49dabc5a7d1413b73681
WHR_EEAS	Kemajou Tchamba, A. L., C. R. Jackson (2025). AIMS_SE_Approach2_WHR_EEAS, HydroShare, http://www.hydroshare.org/resource/b4dafa88679a444da26261d4c47ee784





Table A2: Summary of extracellular enzymes assessed in this study and their associated reactions.

Enzyme	Model substrate	Product	Reaction
β-D-glucosidase	4-MUB-β-D- glucopyranoside	4-methylumbelliferone (MUB)	Hydrolyzes β-1,4 linkages in cellobiose, releasing glucose
	pNP-β-D-glucopyranoside	p-nitrophenol (light yellow)	•
Phosphatase	4-MUB-phosphate	4-methylumbelliferone (MUB)	Hydrolyze phosphomonoesters to release inorganic phosphate
	pNP-phosphate	p-nitrophenol (light yellow)	•
N-acetylglucosaminidase	4-MUB-N-acetyl-β-D- glucosaminide	4-methylumbelliferone (MUB)	Hydrolyzes terminal GlnNAc from chitin oligosaccharides, releasing N-
	pNP-β-N- acetylglucosaminide	p-nitrophenol (light yellow)	- acetylglucasamine
Phenol oxidase	3,4- dihydroxyphenylalanine (L-DOPA)	Dopaquinone (red-brown)	Oxidizes polyphenols to quinones using molecular oxygen as electron acceptor
Peroxidase	3,4- dihydroxyphenylalanine (L-DOPA) + H ₂ O ₂	Dopaquinone (red-brown)	Oxidizes aromatic phenols and amines to quinones using hydrogen peroxide as electron acceptor

Table A3: National Center for Biotechnology Information Sequence Read Archive (NCBI SRA) accession numbers for 16S and ITS sequencing data products.

Watershed	Sequencing Region	Sampling Approach	Year	Accession Number
Piedmont (TAL)	16S	2	2022	PRJNA1289217
	ITS	2	2022	PRJNA1289149
	ITS	2	2023	PRJNA1289189
	16S	3	N/A	PRJNA1288562
	ITS	3	N/A	PRJNA1288519
Appalachian Plateau	16S	2	2022	PRJNA1289217
(PRF)	ITS	2	2022	PRJNA1289149
	ITS	2	2023	PRJNA1289189
Coastal Plain (WHR)	16S	2	2022	PRJNA1289217
	ITS	2	2022	PRJNA1289149





ITS 2 2023 PRJNA1289189

945